Diurnal and day-to-day characteristics of ambient particle mass size distributions from HR-ToF-AMS measurements at an urban site and a suburban site in Hong Kong

Berto P. Lee[1], Hao Wang[2], and Chak K. Chan[1,2*]

[1]School of Energy and Environment, City University of Hong Kong, Hong Kong, China

[2]Division of Environment, Hong Kong University of Science and Technology, Hong Kong, China

Correspondence to: Chak K. Chan (chak.k.chan@cityu.edu.hk)

Abstract. Mass concentration based particle size distributions measured by a high-resolution aerosol mass spectrometer were systematically analyzed to assess long and short-term temporal characteristics of ambient particle size distributions sampled at a typical urban environment close to emission sources and a suburban coastal site representing a regional and local pollution receptor location in Hong Kong. Measured distributions were bimodal and deconvoluted into submodes which were analyzed for day-to-day variations and diurnal variations.

Traffic and cooking emissions at the urban site contributed substantially to particle mass in both modes, while notable decreases in mass median diameters were limited to the morning rush hour. Inorganic particle components displayed varying diurnal behavior, including nocturnal nitrate formation and daytime photochemical formation evident in both modes. Suburban particle size distributions exhibited notable seasonal disparities with differing influence of local formation, particularly in spring and summer, and transport which dominated in the fall season leading to notably higher sulfate and organic accumulation mode particle concentrations. Variations in particle mixing state were evaluated by comparison of inter-species mass median diameter trends at both measurement sites. Internal mixing was prevalent in the accumulation mode in spring at the urban site, while greater frequency of time periods with external mixing of particle populations comprising different fractions of organic constituents was observed in summer. At the suburban site, sulfate and nitrate in the accumulation mode more frequently exhibited differing particle size distributions in all seasons signifying a greater extent of external mixing.

At the urban site, periods of greater submicron inorganic mass concentrations were more likely to be caused by increases in both Aitken and accumulation mode particle mass in summer, while at the suburban receptor location organic and nitrate Aitken mode particle mass contributed more regularly to higher total submicron species mass concentrations in most seasons (spring, summer and winter).

1. Introduction

Apart from mass and chemical composition, the size distribution of fine particles represents a vital physical property with important implications for human health and environmental effects of ambient aerosols (Seinfeld and Pandis, 2006). Particle size relates directly to the aerodynamic properties which govern the penetration and deposition of particles in the airways and lungs (Davidson et al., 2005) as well as the scattering and absorption of light which affect the radiative properties and hence ambient visibility (Ahlquist and Charlson, 1967;Bohren and Huffman, 1983;Charlson et al., 1991;Schwartz, 1996;Seinfeld and Pandis, 2006). Hygroscopic growth in response to changes in ambient humidity can alter particle light scattering properties (Seinfeld and Pandis, 2006;Köhler, 1936) and activation of condensation nuclei particles into cloud droplets depend on atmospheric conditions, chemical composition, mixing state as well as the size and morphology of particles (Abbatt et al., 2005;Kerminen et al., 2012;Meng et al., 2014;Westervelt et al., 2013).

Studies into the size distribution of ambient particulate matter in Hong Kong have been largely based on size-segregated filter samples (Yao et al., 2007b;Zheng et al., 2008;Zhuang et al., 1999;Huang et al., 2014;Bian et al., 2014) and measurements by electrostatic classifier instruments (Cheung et al., 2015;Yao et al., 2007a) and were hence either limited in size resolution (offline filter samples) or chemical resolution (total particle count by classification). Most measurements in Hong Kong were conducted in suburban environments. Inorganic ammonium and sulfate were mainly found in fine mode particles in condensation and droplet mode size ranges, while nitrate had strong coarse mode contributions (Zhuang et al., 1999). Seasonal differences were evident in solvent-extractable organics and trace metals which were mainly found in $PM_{0.5}$ particles in the wet season and winter whereas in fall a shift to larger particles (0.5–2.5 μm fraction) in fall indicated a possibly stronger influence of aged particle components in the transition period of the Asian monsoon (Zheng et al., 2008). Size distributions acquired by a fast mobility particle sizer at the suburban HKUST supersite were investigated more recently to study the formation and accumulation of ultrafine particles under different air flow regimes. Particle number concentration enhancements during the day were attributed to secondary formation, while evening and nighttime peaks were thought to be related to transport of aged aerosols from upwind locations. Nucleation mode particle peaks were often observed in fall and related to regional pollution influence (Cheung et al., 2015). New particle formation events at the same site occurred as single and two-stage growth processes with organics and sulfuric acid contributing mainly to first stage growth in the daytime while nighttime second stage growth was attributed to ammonium nitrate and organics. Particle size growth into the diameter range of cloud condensation nuclei (CCN) was typically only achieved with the second growth stage (Man et al., 2015).

Investigations into particle size distributions in urban areas of Hong Kong are even scarcer. Yao et al. (Yao et al., 2007a) studied the properties and behavior of particles in vehicle plumes and reported a competing process between ambient background particles and fresh soot particles in the condensation of gaseous precursors and a dependency on temperature with bimodal volume size distributions observed at lower ambient temperatures and unimodal distributions in the lower accumulation size range at higher ambient temperatures.

The Aerodyne aerosol mass spectrometer (Canagaratna et al., 2007) is widely used to determine the chemical composition of major organic and inorganic components of non-refractory submicron particulate matter (NR-PM_1). In contrast to most traditional aerosol sizing instruments, the AMS is capable of resolving main chemical constituents

67 within size distributions through analysis of particle flight times and particle ensemble mass spectra (Canagaratna et
68 al., 2007;Jayne et al., 2000;Jimenez et al., 2003;Rupakheti et al., 2005) and thus yields valuable additional information
69 on differences in composition of submicron particles with the gross of particle mass in the Aitken mode range ($D_p \sim$
70 10-100nm) and the accumulation mode range ($D_p \sim$ 100-1000nm) covered by the AMS. Thus far most studies
71 employing ambient size distribution data from aerosol mass spectrometer measurements investigated longer time
72 period averages, i.e. campaign averages (Salcedo et al., 2006;Sun et al., 2009;Aiken et al., 2009;Huang et al.,
73 2010;Takegawa et al., 2009;Saarikoski et al., 2012;Li et al., 2015) or specific time periods of interest (Elser et al.,
74 2016;Lee et al., 2013). Mohr et al. separated organic particle mass size distributions by periods of dominant influence
75 of different PMF-resolved organic aerosol factors to study the properties of mass size distributions in relation to
76 organic aerosol composition (Mohr et al., 2012). The 3D-factorization technique is an extension of traditional AMS
77 PMF analysis on organic aerosol allowing to obtain estimates on the size distributions of organic aerosol factors,
78 however under the assumption that factor size distributions remain invariant over the measurement period (Ulbrich et
79 al., 2012).

80 The temporal evolution of species-specific size distributions, are mostly discussed qualitatively (Drewnick et al.,
81 2005) and only few studies have evaluated temporal trends in mass size distributions in greater detail.
82 Particle nucleation and subsequent growth events were investigated in Pittsburgh using size data from an AMS and
83 two SMPS as well as various gaseous pollutant instruments and meteorological information. The AMS mass size
84 distributions were evaluated quantitatively using the time series of binned particle concentrations generated from the
85 grouping of raw data into wider size bins to represent different stages in the particle growth process. (Zhang et al.,
86 2004). The same method was employed to evaluate contributions of ultrafine mode and accumulation mode particles
87 to total organic particle mass (Zhang et al., 2005) by summation of size bins in the range of 30-100 nm and 100-
88 1000nm. The authors also explored diurnal changes in size distributions of particle species by averaging over 3h
89 periods in the morning (6–9 am) and afternoon (1–4 pm). Sun et al. present a qualitative discussion of diurnal
90 variations in the mass size distributions of the m/z 44, m/z 57 and derived $C_4H_9^+$ ion signals from measurements at an
91 urban site in New York (Sun et al., 2011). Similarly, Setyan et al. examined diurnal changes in the mass size
92 distributions of organics and sulfate qualitatively and used binned concentrations (40–120, 120–200, and 200–800)
93 nm in their quantitative analysis to study the evolution of particle chemistry in new particle formation and growth
94 events (Setyan et al., 2012).

95 In this work, we introduce a systematic approach of assessing temporal variations in AMS mass-based particle size
96 distributions from hourly diurnal variations to 24h-average based day-to-day trends to utilize two key instrumental
97 advantages, i.e. species segregation and high time resolution, to obtain a more detailed and quantitative understanding
98 of the variabilities in ambient particle mass size distributions and to provide an additional dimension to standard AMS
99 data analysis techniques. In this context, we present a detailed discussion of particle size data from HR-ToF-AMS
100 measurements during two field campaigns in Hong Kong in both urban and suburban environments. We aim to
101 evaluate characteristic recurrent changes in size distribution as well as longer term trends in different seasons by
102 analyzing day-to-day variations and diurnal variations of size distributions of submicron organics, sulfate, and nitrate
103 particle mass. The two contrasting sites represent a typical urban source environment (inner-city, roadside station)

104 close to primary emission sources and a suburban location (coastal, HKUST supersite) which is largely a downwind
105 receptor of varying amounts of local urban, regional and long-range transported pollutants (Li et al., 2015;Huang et
106 al., 2014).

107

2. Methodology

2.1. Field campaigns

110 Sampling of ambient submicron non-refractory particulate matter (NR-PM$_1$) was carried out using an Aerodyne HR-
111 ToF-AMS at the HKUST air quality supersite covering four seasons between May 2011 and February 2012 (spring:
112 2011-05, summer: 2011-09, fall: 2011-11&12, winter: 2012-02). The HKUST supersite is located on the campus of
113 the Hong Kong University of Science and Technology (22°20'N, 114°16'E), on the east coast of Hong Kong in a
114 suburban area with few primary emission sources in the immediate vicinity. Sampled air was drawn from the rooftop
115 of a pump house building at an approximate height of 25m above ground level. For detailed descriptions of the
116 experimental setup, operating conditions, data treatment, and overall species composition we refer the reader to
117 previous publications (Lee et al., 2013;Li et al., 2015;Li et al., 2013). A further sampling campaign took place between
118 spring 2013 (2013-03 to 2013-05) and summer 2013 (2013-05 to 2013-07) at an inner-city urban location in the
119 densely populated and built-up Kowloon peninsula. Measurements were conducted next to the roadside air quality
120 monitoring station (AQMS) operated by the Environmental Protection Department (EPD) of the HKSAR Government
121 in the Mong Kok (MK) district on a pedestrian crossing at a major road junction. Sampled air was drawn from a height
122 of 3m above ground level. A comprehensive analysis of trends in species concentration and composition identified in
123 this urban campaign has been presented previously (Lee et al., 2015). In both campaigns, particles were sampled
124 through a PM$_{2.5}$ cyclone at a flow rate of 16.67 L/min into a sampling port from which 0.08 L/min was drawn by the
125 AMS and the remainder drawn by co-sampling instruments and an auxiliary pump. Sample air for the AMS passed
126 through a 1m long diffusion dryer (BMI, San Francisco CA, USA) filled with silica gel to remove bulk gas- and
127 particle-phase water. Additional data from various collocated instruments including meteorological data (wind,
128 temperature, relative humidity, solar irradiation), volatile organic compounds (VOCs) and standard trace gases such
129 as NO$_x$, SO$_2$, and O$_3$ were available.
130 AMS data were treated according to general AMS data treatment principles (DeCarlo et al., 2006;Jimenez et al., 2003)
131 with standard software packages (SQUIRREL, PIKA). Analysis of the unit-mass resolution mass spectra yielded non-
132 refractory submicron particle species concentrations of major inorganic constituents (SO4, NO3, NH4, Chl) and total
133 organics at a base time resolution of 10 min. Positive Matrix Factorization (PMF) was used to deconvolute high-
134 resolution organic mass spectra acquired at 10 min time resolution following recommended PMF guidelines for AMS
135 data (Zhang et al., 2011) with the AMS PMF analysis toolkit (Ulbrich et al., 2009). At the urban Mong Kok site, six
136 organic aerosol (OA) factors were identified encompassing three secondary organic aerosol (SOA) and three primary
137 organic aerosol (POA) factors of which one was attributed to traffic emissions and two to cooking activities (Lee et
138 al., 2015). Similarly, four factors were obtained from analysis of the urban HKUST site dataset with two SOA factors

139 and two POA factors, related to traffic and cooking respectively (Li et al., 2015). Further details on the treatment of

140 AMS size distribution data from both sampling campaigns are provided in the following section.

2.2. Data acquisition and treatment

142 In both campaigns, mass concentration based size distributions in terms of vacuum-aerodynamic particle diameter

143 (dM/$d$logD$_{va}$) were established by joint acquisition of particle time-of-flight (PToF) measurements and unit mass

144 resolution mass spectra (V-mode) with alternation between modes every 20s for 30 cycles amounting to 5 min of total

145 sampling time. High-resolution mass spectra were acquired for the following 5 min, and thus the overall raw data time

146 resolution for each mode was equal to 10 min. The total particle mass measured in the PToF mode was normalized to

147 the V-mode mass concentration of the same time step. Daily size distributions were generated by averaging over 24h

148 periods (from 0:00 to 23:59). Hourly diurnal size distributions were reconstructed by grouping size distributions within

149 the same hour of the day and establishing representative size distributions based on average, median, 25th and 75th

150 percentile concentration values of each size bin (*referred to as size distribution sets hereinafter*).

151 At both sampling sites, the seasonally averaged AMS size distributions were bimodal (Lee et al., 2013, 2015;Li et al.,

152 2015) with similar distributions having been observed in other AMS field studies in various parts of the world. (Zhang

153 et al., 2014;Sun et al., 2011;Huang et al., 2011;Aiken et al., 2009;Zhang et al., 2005;Crippa et al., 2013;Docherty et

154 al., 2011;Mohr et al., 2012). Multimodality of size distributions is typical for environments where different sources or

155 formation processes of particles play a role and accordingly such distributions can also be represented as sums of

156 discrete lognormal distributions of the respective constituting submodes (John, 2011).

157 The measured bimodal size distributions in this work were deconvoluted by fitting two log-normal distributed modes,

158 including one closer to the Aitken size range (*mode diameter ~100nm*) and one in the accumulation size range (*mode

159 diameter ~500nm*) employing the Levenberg-Marquardt algorithm (Gill et al., 1981) as a non-linear least squares fit,

160 to evaluate differences in trends and formation or transformation processes in the two size regimes. An example of a

161 size distribution fit and associated parameters is depicted in Figure D1 in the Supporting Material. Additional fit

162 residual analyses were carried out in cases where the Aitken mode only accounted for small parts of (<10%) of the

163 total particle mass and uncertainties in integrated mode particle mass from the peak fitting were examined for all size

164 distributions. Details are presented in Section B of the Supporting Material. The smaller mode typically exhibited

165 mode diameters in the range of 100-200 nm (D$_{va}$) and is thus in the transition region between Aitken and lower

166 accumulation mode. For a clearer distinction from the larger mode which unambiguously belonged to the

167 accumulation size range, we opt to refer to the small mode as *Aitken mode* in this work. Mode diameter (*i.e.* mass

168 median diameter, MMD), curve width (*i.e.* geometric standard deviation, GSD) and curve area (*equivalent to particle

169 mass concentration within the mode*) are sufficient parameters to completely describe a lognormal distribution and

170 these key variables are used in the following analysis on trends in the fitted species-specific size distributions of

171 organics, nitrate, and sulfate from both HR-AMS sampling campaigns in Hong Kong. Particle diameters are discussed

172 in terms of vacuum-aerodynamic diameter, with detailed discussions on properties and relationships to other size

173 metrics available elsewhere (DeCarlo et al., 2004;Slowik et al., 2004). Further details on procedures of PToF data

174 acquisition and size distribution averaging can be found in the Supporting Material in Section A and B respectively.

175 The sequence of main data treatment and analysis steps is shown in Figure 1.

176 The transmission efficiency of the AMS aerodynamic lens is known to fall off below ~100nm and beyond ~550 nm

177 of vacuum-aerodynamic diameter (Liu et al., 2007;Takegawa et al., 2009;Zhang et al., 2004;Bahreini et al.,

178 2008;Williams et al., 2013;Knote et al., 2011) and may bias measured particle mass and mode diameters, particularly

179 in the accumulation mode towards lower values if significant particle mass fractions fall in the size region of $D_{va} >$

180 550 nm. In the Aitken mode range, the effect of limited lens transmission is expected to be less substantial as particle

181 volume (and hence particle mass) of Aitken mode particles are much smaller. We discuss the effects of lens

182 transmission briefly in section 3.4. Delayed vaporization of particle components, e.g. under high mass loadings, can

183 lead to small shifts towards larger mode diameters in AMS size distributions (Docherty et al., 2015) and enhanced

184 tails in the size distributions (Cross et al., 2009), which may lead to larger fit residuals at the trailing edges. Generally,

185 the discussion of size distributions in this work should be viewed in the context of the instrumental capabilities and

186 previously mentioned limitations of aerosol mass spectrometry. Therefore, the resolved Aitken and accumulation

187 modes in this work reflect the apparent Aitken and accumulation modes within AMS measurable particle mass size

188 distributions.

189
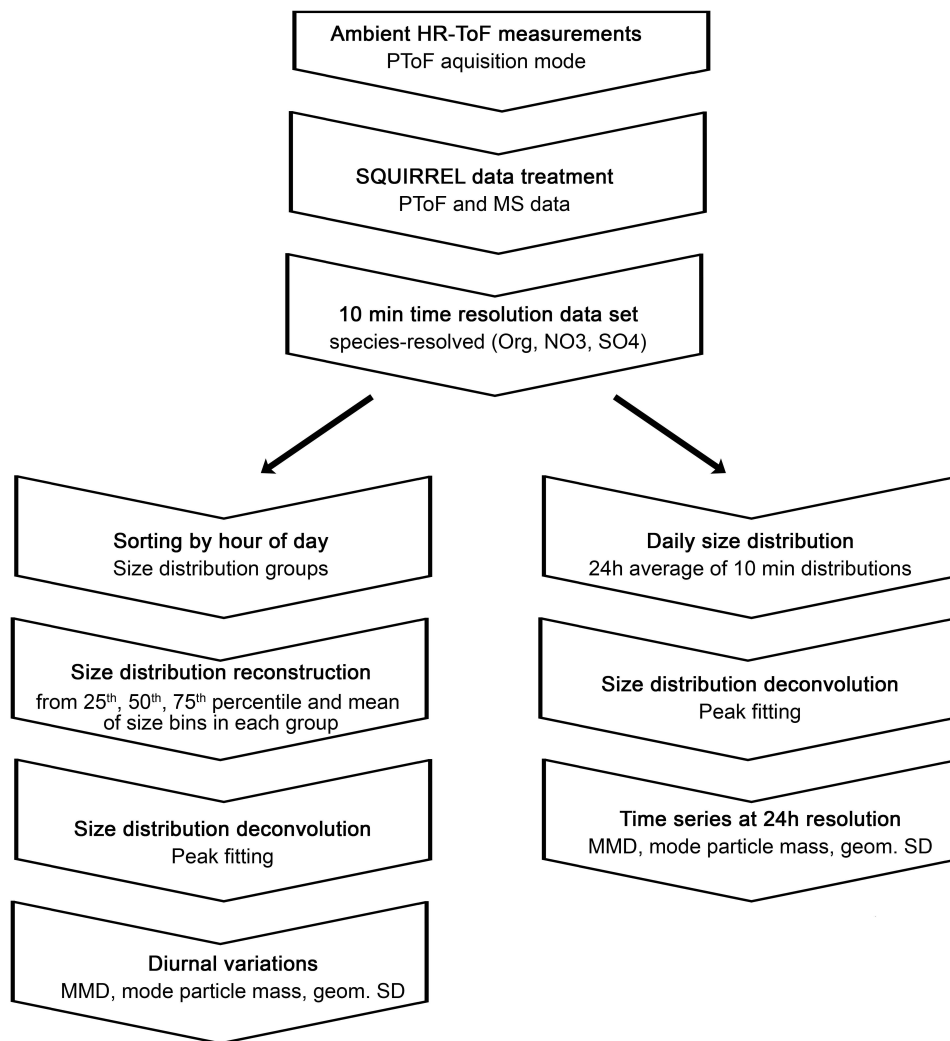
190

191 **Figure 1.** Flow chart of main data acquisition, data treatment and data analysis procedures

3.   Results and Discussion

3.1. Diurnal size distribution characteristics

Diurnal species variations are predominantly discussed in terms of total mass concentration up to the size cut of the sampling inlet or the instrumental capability, e.g. total species concentrations in NR-PM$_1$ for AMS-based studies. AMS mass-based size distributions can be utilized more systematically and complementary to standard AMS data analysis techniques by deconvoluting multimodal distributions into their constituting submodes and evaluating their variation and contribution to overall species concentration variations on a diurnal time scale. As previously mentioned, we examined size distributions reconstructed from the average, median, 25th and 75th percentile of hourly grouped size distributions, analogous to commonly reported AMS species diurnal variations, with quantitative analysis focusing on concentrations from the median dataset.

3.1.1. Urban roadside NR-PM₁

The urban roadside measurements took place between March and July 2013 covering two seasons (Spring 2013: *March to mid-May 2013;* Summer 2013: *mid-May to July 2013*) at a location dominated by the influence of primary emission sources. Organics were the major particulate species in NR-PM₁ of which two-thirds were attributable to traffic and cooking sources. Anthropogenic gas-phase species, including various VOCs, NOₓ, CO, and SO₂ were continuously abundant as well (Lee et al., 2015;Sun et al., 2016). Particle size distributions at the urban site exhibited discernible diurnal trends, with Figure 2 depicting the variations in (mass median) diameters of the lognormal fitted Aitken and accumulation modes, corresponding integrated peak areas representing the total mass accounted for by particles in each mode, the geometric standard deviation signifying the spread across particle sizes as well as the total submicron mass (NR-PM₁) diurnal variation for organics, sulfate, and nitrate based on AMS V-mode data. Individual trends are discussed species-wise in the following.
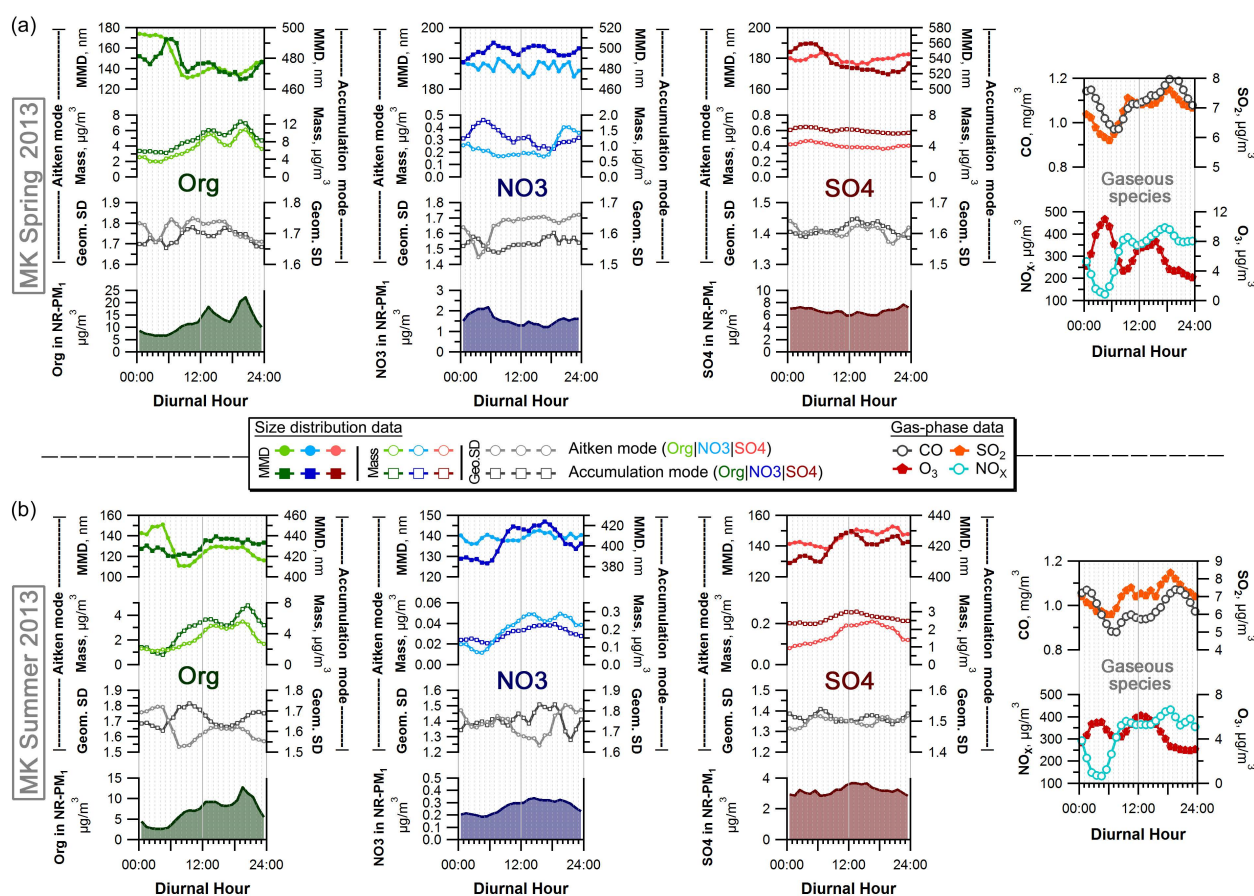
Figure 2. Diurnal variations of mode diameter (MMD), integrated mode mass concentration and width of the Aitken mode (*lighter color*) and accumulation mode (*darker color*) from bimodal peak fits of the bin-median reconstructed size distributions at the urban Mong Kok site and V-mode AMS species concentrations (*line with shaded background*) for organics, nitrate and sulfate (*left to right*) in (a) Spring 2013 and (b) Summer 2013; The right-most panel depicts the median diurnal variations of relevant gas-phase pollutants (O₃, CO, NOₓ, SO₂) measured at the adjacent Mong Kok Air Quality Monitoring Site (MK AQMS)

 Organics

The diurnal variation of total Aitken and accumulation mode particle mass both largely followed the same trend as total submicron organic mass (lower panels in Figure 2 a, b) affirming that urban sources of organic particulate matter contributed substantially to PM mass across the covered size region. Mass concentrations in both modes were smallest during the night (*0:00 to 6:00*) and highest during lunch and dinner (*12:00 to 14:00, 19:00 to 21:00*), when the influence of organic aerosol from cooking (COA - cooking organic aerosol) and from traffic (HOA – hydrocarbon-like organic aerosol) were dominant (Lee et al., 2015). Trends in integrated mode particle mass and MMDs were similar across all size distribution sets (Figure D6 in the Supporting Material), confirming that they occurred persistently throughout the measurement period and making diurnal timescale processes the dominant factor in determining size characteristics of organic-containing particles at this urban roadside location.

Minimum Aitken mode particle mass concentrations (*median values*) amounted to 2.3 µg/m^3 in spring and 1.2 µg/m^3 in summer, accounting for 28-38% of total submicron particulate mass, and were typically reached between 03:00 and 04:00. These concentrations represent the estimated urban background mass of Aitken mode particles carried over from the daytime and not removed by gravitational settling, coagulation or sweep-out as well as contributions from nighttime activity such as traffic, which remains continuous in the inner-city districts at night albeit at much lower vehicle numbers compared to the daytime.

Organic concentrations increased notably between 6:00 and 9:00 during the morning rush hour with traffic-related constituents (*HOA – hydrocarbon-like organic aerosol*) accounting for the largest part (60% in spring, 40% in summer) of this increase. In the Aitken mode, particle mass concentrations rose by 1.6 µg/m^3 (spring) and 0.8 µg/m^3 (summer) in the same time period. Assuming direct proportionality between the contribution of HOA to total submicron organic mass increase and the increase of particle mass in each submode, 0.9 µg/m^3 (spring) and 0.3 µg/m^3 (summer) of particle mass were estimated as traffic-related organic components in the Aitken mode. Significant changes were evident in the particle size metric (MMD) during the same time period, where a consistent decrease by 20-30% from about 170 nm (spring) or 160 nm (summer) to 130-140 nm (spring) or 120 nm (summer) was evident with the concurrent increase in road traffic. This combined shift to smaller particle size and increase in total particle mass denotes a strong increase in the total number concentrations of particles in the Aitken mode range by at least a factor of 4-5 (assuming spherical particles and constant particle density) with significant additional contributions expected from elemental carbon particles and smaller Aitken mode and nucleation mode particles below the range of efficient particle transmission of the AMS inlet lens (Williams et al., 2013).

Beyond 10:00, changes in submicron organic mass concentrations were dominated by variations in cooking-related organic aerosol (COA) components. During the main meal times (12:00 – 14:00 and 19:00 – 21:00) changes in organic submicron mass were almost entirely (>80%) caused by COA in both seasons (Table C4 in the Supporting Material) and daily maximum Aitken mode particle mass concentrations typically occur during these hours (5.5 – 6.2 µg/m^3 in spring, 3.1 – 3.5 µg/m^3 in summer) with higher concentrations during the dinner period. Analogous to HOA, considering proportionality between COA fractional contribution and submode particle mass increase, primary cooking emissions accounted for 1.7 - 1.8 µg/m^3 of organic particle mass in the Aitken mode. Dinner in summer represents a notable exception, where the estimated cooking-related increase only amounted to 0.5 µg/m^3. This is

256 mainly due to specific local meteorological and geographical features owing to a greater frequency of easterly surface
257 winds in the warmer season and the geographical distribution of cooking sources predominantly to the east of the
258 sampling site (Sun et al., 2016;Lee et al., 2015), which led to considerably elevated Aitken mode mass concentration
259 throughout the day including the late afternoon period and a correspondingly smaller additional increase during the
260 dinner time. The aforementioned effect is particularly evident in the diurnal trend of the Aitken mode particle mass
261 fraction among total organic submicron mass (Figure 3a) which displayed a broad bell-shape during the day in summer
262 with nominal increases of 9-10%, whereas in spring the variation follows a double peak behavior with nominal
263 increases of 4-5% during the meal times which emphasize the more intermittent behavior of cooking-related particle
264 contributions in spring. Cooking emissions did not lead to conspicuous changes in the size-related distribution metrics,
265 i.e. there were no obvious trends in particle diameters (MMDs) or distribution widths (GSDs) during the meal time
266 periods (Figure 2a, b - *black lines in lower panels*).

267 In the accumulation mode, organic particle mass during the night hours (00:00 – 06:00) was 2.5 times larger in spring
268 (5.5 µg/m^3) than in summer (2.0 µg/m^3). The mass concentration increase during the morning rush hour was larger
269 in summer (ΔM=3.9 µg/m^3) than in spring (ΔM=3.0 µg/m^3), which was mainly caused by daytime increases of SOA
270 components in summer (Lee et al., 2015), and consequently led to a lower fractional rush hour increase of traffic
271 related organic constituents. Estimated particle mass contributions of traffic emissions in the accumulation mode
272 amounted to 1.8 µg/m^3 in spring and 1.6 µg/m^3 in summer. In terms of particle size, the onset of the rush hour had
273 little conspicuous effects on the accumulation mode without clear trends in MMDs in both seasons. In summer the
274 shift to smaller MMDs was accompanied by a notable narrowing of the Aitken mode, whereas in spring Aitken mode
275 distribution widths remained largely stable throughout the day (Figure 2a, b - *lower panels*).

276 Maximum accumulation mode particle concentrations during the meal hours reached 10.5 – 12.3 µg/m^3 in spring and
277 6.0 – 7.4 µg/m^3 in summer. Analogous to the Aitken mode, estimated cooking-related particle contributions in the
278 accumulation mode amounted to 2.0 µg/m^3 (spring) and 1.0 µg/m^3 (summer) during lunch, and to 2.7 µg/m^3 (spring)
279 and 2.4 µg/m^3 (summer) during dinner. Also, distribution widths (GSD) in the accumulation mode were not notably
280 affected by cooking emissions. Seasonal differences were apparent in the mass median diameters of the accumulation
281 mode. In spring, mode diameters remained largely constant (+/- 10nm) apart from a subtle peak during the morning
282 rush hour, indicative of minor condensational growth of traffic-related primary organics or rapidly formed secondary
283 species. In summer, a consistent increase in particle size by 20nm (~5%) during the daytime points to particle growth
284 through secondary formation as a governing factor.

285 Aitken mode particles contributed larger fractions to the total increase in organic submicron particle mass during the
286 rush hour and mealtimes in spring (33-56%) than in summer (16-38%). These differences were presumably due to
287 seasonal meteorology and associated effects on the formation, accumulation, and dispersion of particles from primary
288 emission sources, as source strengths and characteristics of road traffic and commercial cooking are unlikely to vary
289 with seasons in the inner-city urban areas of Hong Kong. Ambient temperatures and solar irradiation differed
290 substantially with 7°C higher average temperatures and three times higher integrated daily solar irradiation in summer
291 compared to spring (Figure D10e-f in the Supporting Material). Lower overall ambient temperatures enhance
292 condensation of gas-phase emissions and particle nucleation and shift the gas-to-particle partitioning equilibrium of

293   semi-volatile constituents towards the particle-phase. We expect these volatility effects to be a main contributing

294   factor, as sampling took place in direct vicinity of the emission source, i.e. next to the road and thus potential impacts

295   of physical effects such as enhanced near-ground mixing and dispersion through thermally induced convection in

296   summer are expected to be of minor influence. Considering the previously discussed estimated traffic contributions

297   during the rush hour, the seasonal difference in mass concentration was much more pronounced in the Aitken mode

298   (-67%, 0.6 µg/m^3) than the accumulation mode (-12%, 0.2 µg/m^3), consistent with the expected stronger impact of

299   reduced particle nucleation and reduced condensation of semi-volatile exhaust components on fresher, smaller

300   particles in the warmer season.

301   Comparing different size distribution sets (Figure D6 in the Supporting Material), the average concentration set in

302   summer yielded notably larger resolved mass median diameters in both modes and greater Aitken mode mass

303   compared to the median, 25th, and 75th percentile concentration sets. This indicates a strong influence of extreme

304   values (i.e. time periods with both larger particle size and larger particle mass concentrations) and thus greater

305   variability in size distributions in the warmer season caused by specific high and low concentration events such as

306   photochemical episodes and precipitation, evident in the greater relative span of organic mass concentrations in

307   summer (See Table C5 in the Supporting Material: ratio of 10th and 90th percentile to median concentration in NR-

308   PM$_1$). In spring, such events masked the diurnal processes to a lesser extent and with consequently greater consistency

309   across different size distribution sets.

310

311   Sulfate

312   Although variations of total submicron sulfate mass concentrations with time of day were generally subtle, distinct

313   trends were notable in MMDs and integrated mode mass concentrations in both Aitken and accumulation mode.

314   Generally, Aitken mode MMDs were 20% larger in spring (180nm) than in summer (150nm). While in spring

315   fluctuations in Aitken mode MMDs were small throughout the day within a narrow range of +/- 10nm and without

316   apparent regular features, the summertime diurnal variation exhibited a well-defined broad daytime peak with a shift

317   to ~15nm larger particle diameters. A matching trend was evident in the accumulation mode where MMDs increased

318   by ~20nm in summer. Conversely, in spring, a conspicuous nighttime peak in accumulation mode MMDs was

319   observed in the low traffic period between 01:00 and 07:00 which tracked closely with the diurnal variation of O$_3$

320   which peaked in the same period with the reduction of the NO$_x$ titration effects at low nighttime traffic volumes. While

321   particulate sulfate production during the day can be achieved through both homogeneous gas-phase oxidation of SO$_2$

322   by the OH radical as well as heterogeneous oxidation of SO$_2$ by dissolved H$_2$O$_2$ or O$_3$ (Seinfeld and Pandis, 2006),

323   nighttime production is limited to the non-photochemical heterogeneous pathway. The apparent increase in

324   accumulation mode particle size was also associated with an increase of integrated submode particle mass by ~0.7

325   µg/m^3 and thus suggests the possibility of heterogeneous SO$_2$ oxidation by residual ozone in the cooler and more

326   humid spring season as a local source of particulate sulfate. In the warmer and drier summer season, no corresponding

327   trend was apparent in either accumulation mode MMD or integrated mode concentration. The small magnitude of

328   additionally produced sulfate (< 1 µg/m^3) in spring renders the nighttime production a minor source of particulate

329   sulfate however and affirms that the bulk of the accumulation mode sulfate burden at the urban roadside still originated

330 from regional scale processes in both seasons. In summer, both modes exhibited notable increases in particle mass
331 concentration levels during the daylight hours by ~80% in the Aitken mode and by ~35% in the accumulation mode
332 compared to their respective nighttime "baseline" concentrations. Integrated over the whole day, the additional sulfate
333 burden above this baseline amounted to 0.4 µg/m^3 and 6 µg/m^3 and thereby accounted for 34% and 11% of the total
334 daily Aitken and accumulation mode particle mass respectively. This represents a rough estimation of possible local
335 photochemical contributions to the Aitken and accumulation size mode in summer at the urban roadside, excluding
336 possible physical effects, e.g. vertical mixing and advection or dilution laterally through the street canyon.
337 Enhancements in particle mass by photochemical contributions were more pronounced in the Aitken mode, with the
338 median fraction of Aitken mode particle mass among total AMS-measured particle mass increasing substantially from
339 its nighttime minimum at 4% to a maximum of 7% in the late afternoon in summer, while in spring the fraction
340 remained almost constant at 6% throughout the day (Figure 3a).
341 Considering different size distribution sets (Figure D6 in the Supporting Material), the 75th percentile size distributions
342 and the average size distributions displayed notable increases in Aitken mode particle mass during the nighttime by
343 20-50% in spring. There was no corresponding trend in the accumulation mode, where changes in integrated mass
344 concentration remained consistently <10%. The skewing of the average and higher percentile data indicates the
345 influence of time periods with significantly elevated nighttime concentrations, likely related to events and atmospheric
346 conditions conducive to the extensive formation of Aitken mode sulfate particles. The accumulation mode showed no
347 notable changes in the average and 75th percentile data during the same time period, thus precluding physical processes
348 such as transport or lowering of the planetary boundary layer as likely influential factors for these observations.
349
350 Nitrate
351 Particulate nitrate mass concentrations in the Aitken and accumulation mode exhibited similar diurnal variations in
352 spring with lower daytime concentrations due to evaporation and higher nighttime concentrations where secondary
353 formation and gas-to-particle partitioning prevailed. Analogous to sulfate, the Aitken mode MMDs for nitrate showed
354 little change (<5%) throughout the day in both seasons. Aitken mode mass concentrations, however, exhibited a
355 twofold increase over the dinner hours accounting for approximately 0.9 µg/m^3 (~16%) of additional particle nitrate
356 mass per day. This may be due to the much higher abundance of small particles from cooking emissions providing
357 additional surface area to facilitate gas-to-particle partitioning of nitrate. Increased signal intensities of oxygenated
358 organic nitrogen ions (see Figure D11 in the Supporting Material) have also been observed during dinner suggesting
359 that organic nitrate or other oxygenated nitrogen-containing organic species that produce nitrate fragments (Farmer et
360 al., 2010) may too have contributed to this observed concentration peak. Accumulation mode nitrate mass increased
361 by almost one-third in the low traffic period (01:00 – 07:00) compared to earlier night concentration levels (22:00 –
362 00:00) accompanied by a slight increase in MMD by ~10nm in spring. This signifies notable nighttime nitrate
363 production through possibly nitric acid formation by ozone chemistry via the nitrate radical route under influence of
364 organic components or formation of N_2O_5 and subsequent hydrolysis during the night. Local nighttime nitrate
365 production effectively contributed ~3 µg/m^3 (~10%) to the total daily accumulation mode nitrate burden in spring.

Summertime nitrate production in Hong Kong has been mainly attributed to photochemical activity based on previous measurements of inorganic gas- and particle-phase nitrogen species at the suburban HKUST site (Griffith et al., 2015). Particulate nitrate mass concentrations at the urban Mong Kok site likewise exhibited clear daytime peaks, similar to sulfate albeit at smaller magnitude with total integrated increases of ~0.3 µg/m³ and ~0.8 µg/m³ particulate nitrate per day in the Aitken and accumulation mode respectively. In the Aitken mode, particle mass remained elevated in the early night hours (~19:00 – 22:00), which was likely due to the previously mentioned cooking-related nitrate enhancement analogous to spring. The distribution of total submicron nitrate shifted slightly in favor of the Aitken mode in summer with ~18% of total submicron nitrate found in the Aitken mode compared to ~14% in spring. Comparing different size distribution sets (Figure D6 in the Supporting Material), the average size distributions displayed notable disparity compared to the remaining sets in both seasons. In summer, integrated particle mass concentrations and MMDs from the average set exhibited consistently larger values than those from the 25th percentile, 75th percentile, and median sets indicating significant influence of time periods with high nitrate concentrations and larger nitrate-containing particles. In spring, the average data exhibited a decrease in MMD in the Aitken mode from night to day, implying prolonged periods of significantly smaller daytime Aitken mode particles.
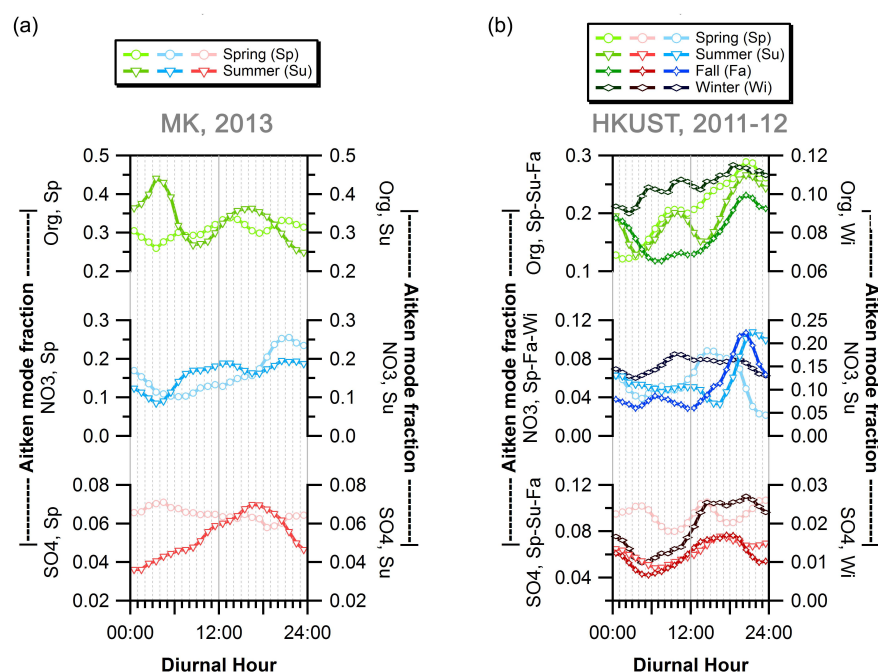
Figure 3. Diurnal variation of the fraction of Aitken mode particle mass among total submicron species mass for organics (*top*), nitrate (*middle*) and sulfate (*bottom*) at the (a) urban Mong Kong site, and (b) suburban HKUST supersite in different seasons; *based on concentrations from bin-median size distributions, seasons denoted by marker color and type of marker symbol*

384
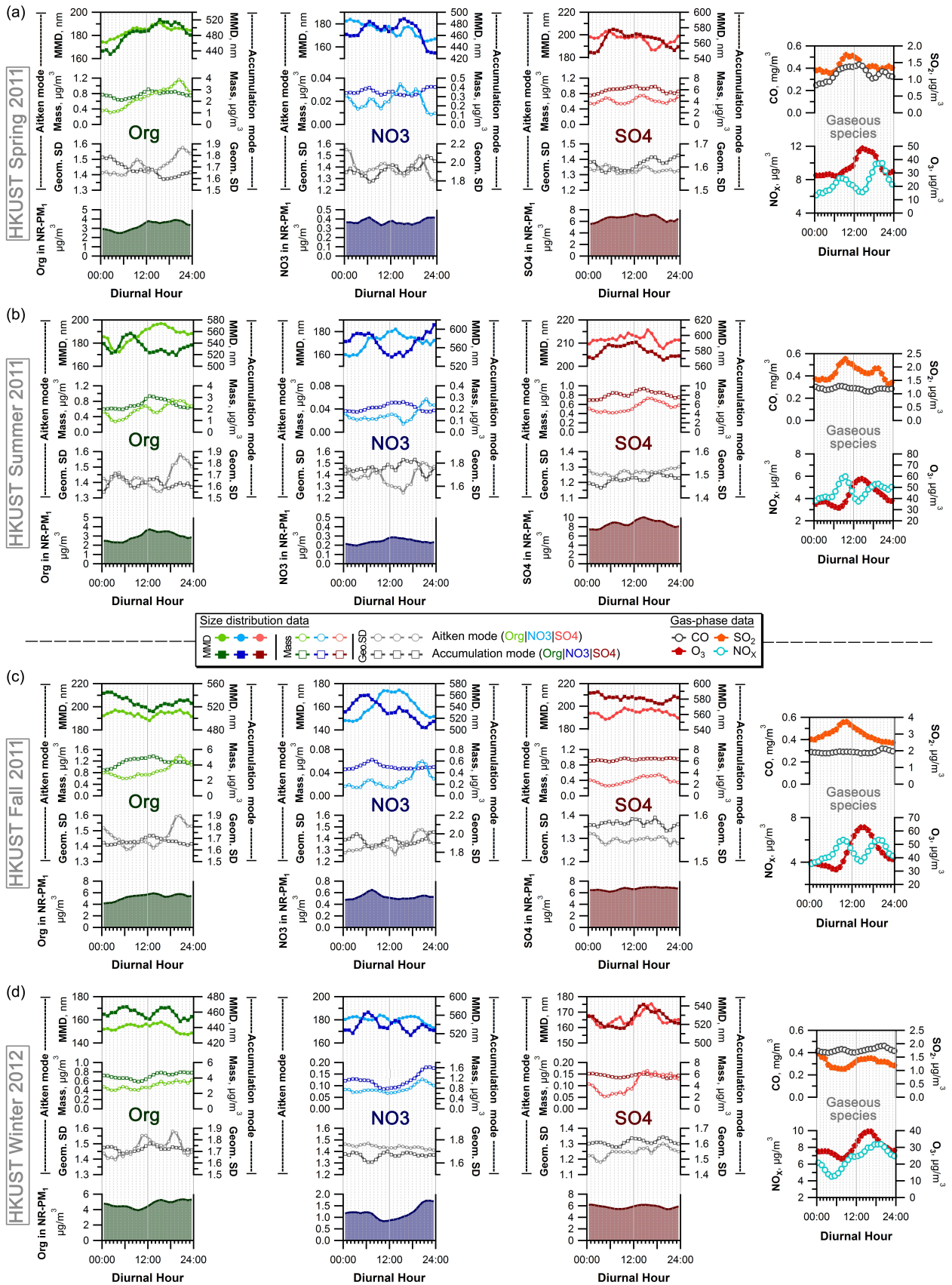
385   **Figure 4.** Diurnal variations of mode diameter (MMD), integrated mode mass concentration and width of the Aitken mode (*lighter*

386   *color*) and accumulation mode (*darker color*) from bimodal peak fits of the bin-median reconstructed size distributions at the

387   suburban HKUST site and V-mode AMS species concentrations (line with shaded background) for organics, nitrate and sulfate

388   (left to right) in (a) Spring 2011, (b) Summer 2011, (c) Fall 2011 and (d) Winter 2012; The right-most panel depicts the median

389   diurnal variations of relevant gas-phase pollutants (O_3, CO, NO_x, SO_2) measured at the same site.

390   ### 3.1.2.   Suburban coastal NR-PM$_1$

391   The suburban HKUST site as a downwind receptor of urban and regional pollution was generally dominated by sulfate

392   and oxygenated secondary organic aerosol (SOA) components and much lower fractions of primary organic

393   constituents, which combined typically made up less than a quarter of total organics (Li et al., 2015). Trends in the

394   species segregated particle size distributions are discussed analogously to section 3.1.1., with Figure 4 illustrating the

395   diurnal trends of the fitting parameters (MMD, integrated mode mass, geometric standard deviation) for organics,

396   sulfate, and nitrate at the suburban HKUST site.

397

398   Organics

399   There were significant seasonal differences with larger fractions (Figure 3b) and concentrations (Figure 5c) of Aitken

400   mode mass in total organic submicron particle mass in spring and summer compared to fall and winter, indicating

401   greater influence of closer-ranged formation sources in the warmer season. Springtime integrated Aitken mode mass

402   concentrations (~0.8 µg/m^3) were twice as high as those in winter (~0.4 µg/m^3). In the accumulation mode, highest

403   particle mass loadings were observed in fall (5 µg/m^3) and lowest loadings in spring (3 µg/m^3) following the frequency

404   pattern of continental air mass influence (Figure D12 in the Supporting Material) in each season indicating continental

405   transport of particulate mass or gas-phase precursors. Lowest mass concentrations in the Aitken mode typically

406   occurred in the night hours (00:00 – 05:00) in a range of 0.3 – 0.5 µg/m^3 in spring, summer, and winter, while in fall

407   mass loadings of 0.7 - 0.8 µg/m^3 were reached. Diurnal changes were least pronounced in winter with largely constant

408   integrated Aitken mode particle concentrations. In the remaining seasons, varying degrees of daytime changes were

409   apparent with a general increase around 06:00, likely owing to citybound commuter traffic from surrounding roads to

410   the west of the sampling site at 1-2km of lateral distance. This also led to a modest increase in particle polydispersity

411   with a discernible widening of the Aitken mode size distributions (*black solid line, lowest panels in* Figure 3). Daily

412   maxima in spring, summer and fall were reached in the early evening (~21:00) with marked differences in absolute

413   mass concentrations depending on the respective season, from a summer time low of 0.8 µg/m^3 to a fall season high

414   of 1.4 µg/m^3. Mass median diameters in the Aitken mode were smaller in the night hours and displayed subtle

415   increments during the day in the range of 10-20 nm reaching their maximum typically in the late afternoon, except for

416   the fall season when mass median diameters displayed very little variation with time of day.

417   Total particle mass in the accumulation mode in spring and summer reached minima during the night hours (2 µg/m^3)

418   and maxima (3 µg/m^3) around noon, remaining stable in the daylight hours thereafter. MMDs increased notably from

419   440nm at night to 510nm during the day in spring, while in summer a morning rise by ~30nm from 530nm to 560nm

420   was obvious between 06:00 and 10:00 and coincided with the morning rush hour and the associated early morning

peak of NO_x and an otherwise stable mode diameter of 530nm for the rest of the day. In fall, the increase in accumulation mode organic mass occurred much earlier, starting in the dark hours at 04:00, with a corresponding trend also evident for nitrate but absent for sulfate, indicating a common source of these organic and nitrate enriched particles. Nighttime MMDs for organics were generally larger (540nm) and decreased to a minimum of 510nm in the early afternoon accompanied by a slight widening of the distribution. In winter, mass concentrations decreased appreciably in the early morning hours and started to increase only beyond 10:00. In the colder seasons (fall, winter), a similar concentration pattern was also observed for gas-phase SO_2 which is considered as a largely regional pollutant with few distinct local sources (Yuan et al., 2013), indicating that changes in boundary layer and mixing with regional background were likely the more dominant processes in winter.

Sulfate

Aitken mode sulfate mass concentrations peaked in the afternoon from spring throughout fall with maximum concentrations reached progressively later in the afternoon (14:00 in spring; 16:00 in fall). Nominal concentrations were highest in spring and summer (0.5-0.6 µg/m^3), slightly lower in fall (0.4 µg/m^3) and reached the lowest levels in winter (0.1 µg/m^3). In addition to the afternoon peak, a conspicuous early morning peak of similar magnitude was evident in spring between 02:00 and 06:00. A greater proportion of southerly winds was evident in said time period compared to the overall seasonal wind frequency distribution (Figure D13a in the Supporting Material) and may indicate transport of sulfate from marine sources in the southern parts of Hong Kong. Diurnal variations in MMDs and GSDs were generally small and without obvious regular trends. Nominal mass median diameters were significantly lower in winter (~170nm) compared to spring and fall (~190nm) and summer (~210nm).

Trends in accumulation mode particle mass were more pronounced. In spring, a shallow concentration valley during the late evening and night hours (20:00 to 03:00) with minimum concentrations of 5 µg/m^3 was apparent, while daytime concentrations stayed largely invariant at 6 µg/m^3. The MMDs followed a similar variation with a minimum mode diameter around 550nm in the early hours of the day and slightly larger daytime MMDs around 570nm. Nominal concentrations were larger in summer with a nighttime valley concentration of 7 µg/m^3 and a well-pronounced broad day peak with a maximum of 9.5 µg/m^3 in the early afternoon (14:00-15:00). A prior additional morning peak occurred between 04:00 and 10:00 with particle mass concentrations reaching 8.5 µg/m^3 related to a consistent north-easterly morning wind pattern (Figure D13b in the Supporting Material) and likely associated with transport from north-easterly coastal regions or nighttime fisheries related maritime traffic. The diurnal trend in mass median diameter was similar to that in spring with a night minimum of 570nm and day maximum of 590nm.

In fall, accumulation mode characteristics showed no significant diurnal variability, with a largely stable integrated particle mass of 6 µg/m^3 and only subtle MMD changes (585nm at night; 575nm during the day). In winter, two concentration dips with reductions by ~0.5 µg/m^3 between 06:00 and 10:00 and between 18:00 and 22:00 were evident, while MMDs increased during the day between 10:00 and 15:00 from 520nm, peaking at a size of 540nm.

Nitrate

Nitrate particle mass in the Aitken mode was generally small from spring throughout fall amounting to 0.01 - 0.06

458   μg/m^3. Winter time concentrations were larger in a range of 0.06 - 0.08 μg/m^3 during the day and 0.10 - 0.12 μg/m^3 in

459   the late evening hours. The latter evening peak centered around 21:00 was evident in most seasons (except spring)

460   and accounted for 12-23% (0.1-0.25 μg/m^3) of total daily Aitken mode nitrate mass burden. Similar to the urban

461   roadside location, these nighttime nitrate peaks coincided with the peak period of organic cooking aerosol

462   concentrations (Figure D14 in the Supporting Material), which were however significantly smaller at the suburban

463   measurement site and mainly attributed to the operation of an on-campus student canteen (Li et al., 2015). Trends in

464   mass median diameters varied between seasons with no discernible trend in winter, a subtle decreasing trend with time

465   of day in spring and broad daytime diameter increases in summer and fall. Solar irradiation in these two seasons was

466   comparatively high (Figure D10b-c in the Supporting Material) indicating that photochemical nitrate production in

467   the Aitken mode may have led to this observed growth in particle size.

468   Integrated particle mass concentrations in the accumulation mode only exhibited subtle variations from spring

469   throughout fall, with essentially constant diurnal concentrations in spring, a subtle daytime peak in summer which

470   accounted for ~ 15% of total daily accumulation mode nitrate (corresponding to 0.7 μg/m^3) and a conspicuous morning

471   peak between 04:00 and 10:00 in fall accounting for ~ 5% of total daily accumulation mode nitrate (corresponding to

472   0.5 μg/m^3). Clearer seasonal differences were evident in the trends of MMDs. In spring, MMDs decreased appreciably

473   over the late evening hours (21:00-0:00) with a concurrent widening of the size distribution (increase in GSD). In

474   summer, accumulation mode diameters decreased during the day by ~40nm with a similar trend in accumulation mode

475   organics. Winter time MMDs exhibited a more complex pattern with larger mode diameters in the early hours (04:00

476   – 10:00) and during the noon-time, and a late-afternoon dip leading to larger spread of intra-day mode diameters

477   ranging from 510nm to 570nm.

478   In comparison to the urban roadside measurements, diurnal particle size characteristics and mass concentrations in the

479   Aitken and accumulation mode were much more variable for all investigated species at the suburban HKUST site,

480   indicating that longer time scale processes and irregular events (transport patterns, local meteorology) were probably

481   more important in governing particle size distribution characteristics than diurnal processes.

482   **3.2. Day-to-day size distributions and seasonal averages**

483   To evaluate the evolution of particle size distributions within seasons, average species-specific size distributions were

484   generated by averaging raw distributions over 24h periods (between 0:00 and 23:59). There was clear long-term

485   variability in both resolved Aitken and accumulation mode MMDs and integrated submode particle mass

486   concentrations for all species (Figures D15-16 in the Supporting Material) and overall seasonal differences which

487   have been briefly addressed in the discussion of the diurnal size distribution variations between seasons. Figure 5

488   depicts the overall average values for all daily fitted MMDs and integrated particle mass concentrations in both the

489   Aitken and accumulation mode at the suburban HKUST and urban MK sites.

490

491

3.2.1. Seasonal trends

For the MK roadside station, particle mode diameters were generally larger in spring than in summer for all three investigated species, but with clear differences in the magnitude of changes among individual species. In the Aitken mode, organics and sulfate displayed a moderate decrease in mode diameter from spring to summer by 7-8% each, while nitrate saw a more significant decrease by 25% from spring to summer. In contrast, accumulation mode MMDs for organics exhibited only a subtle decrease by 5% and more substantial decreases for sulfate and nitrate by 20-22% each. Total Aitken mode particle mass decreases varied strongly: -15% for organics, -36% for sulfate and -67% for nitrate. In the accumulation mode, organics and sulfate exhibited similar relative decreases by 40-46%, while nitrate particle mass reduced drastically by 85%.

At the suburban HKUST site, Aitken mode MMDs of nitrate and organics decreased with the progression of seasons from spring to winter with highest mode diameters observed in spring and summer and appreciable decreases in winter by -9% for nitrate and -25% for organics compared to the warmer seasons. Sulfate displayed a similar winter time decrease in MMD (-15%) and an increase of similar magnitude in the summer season (+13%) compared to spring and fall. Variations in sulfate and organic accumulation mode diameters were minor between spring and fall, while wintertime MMDs were 7-12% lower. Nitrate exhibited an overall higher variability in mass median diameters in the accumulation mode in spring (larger standard deviation) and with on average 10% lower MMDs compared to other seasons. In line with the reduction in Aitken mode MMDs in winter, the integrated Aitken mode particle mass decreased as well, by -16% for organics and almost -75% for sulfate, whereas nitrate contributions remained largely stable throughout the seasons. Organic accumulation mode particle mass was significantly higher in the fall and winter season by factors of 1.6 – 2. Diurnal variations in the degree of oxygenation were least pronounced in these seasons (Li et al., 2015) suggesting that influence of transport in autumn and winter likely dominated over local formation, thus exerting greater effects on particle mass in the larger size mode. Particulate nitrate concentrations were generally low in the accumulation mode from spring through fall, but increased sharply in winter by factors of 3 – 4. Sulfate accumulation mode mass concentrations remained more stable but saw significant summer time enhancements by ~30% likely due to photochemical activity which also led to high concentrations of Ox and a higher degree of oxygenation of organic aerosol among the four seasons (Li et al., 2015).
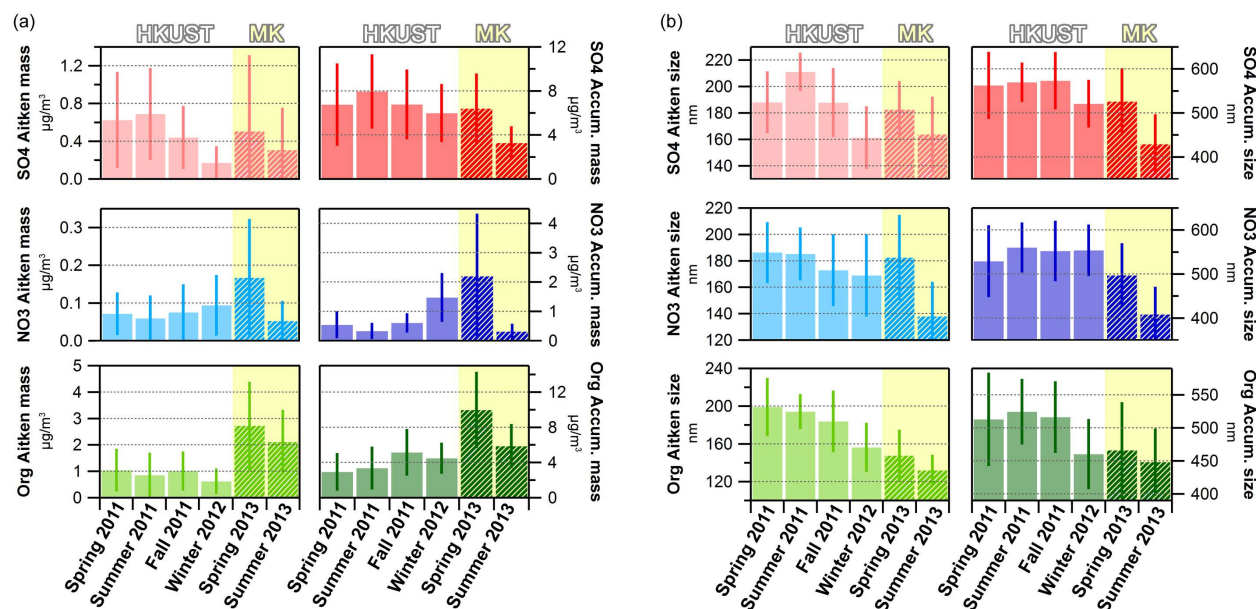
518
519 **Figure 5.** Average and standard deviation of daily fit values of Aitken and accumulation mode particle mass and mass median
520 diameters at the suburban HKUST site (*solid bars*) and urban MK site (*hashed bars*). The integrated particle mass is depicted in
521 (a) for the Aitken mode (*left panels*) and for the accumulation mode (*right panels*) for sulfate, nitrate, and organics respectively.
522 The mass median diameter is depicted in (b) for the Aitken mode (*left panels*) and for the accumulation mode (*right panels*) for
523 sulfate, nitrate and organics respectively.
524
525 Large particles contribute more to particle volume and hence particle mass. Correspondingly, the total submicron
526 concentration of a given species is typically governed by changes in the accumulation mode particle mass and
527 accordingly observed correlation values between integrated accumulation mode particle mass and individual NR-PM$_1$
528 species mass concentrations were generally high (R_{pr}>0.90) at both measurement sites (Figure D17 in the Supporting
529 Material). This applied to both measurement sites regardless of the season. Aitken mode trends were less akin. At the
530 urban roadside station, neither sulfate nor nitrate particle mass in the Aitken mode notably correlated with the
531 respective total submicron species mass concentration in spring (all R_{pr}≤0.20), whereas in summer correlations were
532 more significant with R_{pr}=0.51 for sulfate and R_{pr}=0.80 for nitrate. This signifies that periods of greater species mass
533 concentrations were more likely to be caused by increases in both Aitken and accumulation mode particle mass
534 indicating that particle formation and growth affecting smaller particles was more likely to occur in the warmer season.
535 For organics, Aitken mode particle mass and submicron species mass correlated only weakly (R_{pr} = 0.26 in spring and
536 R_{pr} = 0.38 in summer), i.e. each organic particle submode was governed by largely different dominant sources or
537 formation processes in both seasons at the roadside.
538 At the suburban background site, Aitken mode particle mass for sulfate showed little correlation with total submicron
539 sulfate concentration (R_{pr}≤0.10) apart from the spring season (R_{pr}=0.36) where more frequent wet and foggy
540 conditions may have facilitated sulfate formation in both size modes. For organics and nitrate significantly larger
541 correlation coefficients of submode particle mass to total species concentration ($0.5 \leq R_{pr} \leq 0.7$) were observed in
542 most seasons (spring, summer, winter) indicating significant influence of local or regional formation processes on

543 organic and nitrate Aitken mode particulate mass at the suburban receptor location. In the fall season, much weaker

544 correlations ($0.2 \leq R_{pr} \leq 0.4$) were likely caused by the dominance of continental air mass influence (Figure D12c in

545 the Supporting Material) and greater influence of aged accumulation mode particles on total submicron nitrate mass

546 concentrations.

547 **3.2.2. Inferred changes in mixing state**

548 Shifts in mixing state of ambient particles can be inferred from the inter-species analysis of mass median diameters.

549 Close nominal agreement (i.e. diameter ratios close to 1) infer that different species were distributed similarly across

550 the particle size range which thus most likely represents a largely internally mixed particle population, while the spread

551 of data (correlation coefficient) indicates the temporal homogeneity or divergence of resolved mode diameters. A

552 hypothetically perfectly internally mixed particle population over the whole sampling period would, therefore, yield

553 MMD ratios and Pearson's R values of 1 between species, while larger or smaller values are indicative of a greater

554 frequency of heterogeneous (i.e. more externally mixed) particle populations (Figure 6).

555 At the urban Mong Kok site, changes in accumulation mode mass median diameters for nitrate and sulfate followed

556 similar trends (R_{pr} = 0.88-0.89) and with diameter ratios close to 1 (0.94–0.95) Similarly, fitted accumulation mode

557 diameters of organic constituents predominantly followed that of sulfate in spring nominally (diameter ratio 0.88) and

558 temporally (R_{pr} = 0.80). The nominal agreement of organic and sulfate accumulation mode diameters persisted

559 (diameter ratio 1.03) overall in summer, however, there was significantly more temporal divergence (R_{pr} = 0.65)

560 indicating a greater frequency of time periods with external mixing of particle populations comprising different

561 fractions of organic constituents.

562 External mixing is more prevalent for freshly formed smaller particles which have typically undergone less

563 condensational growth, coagulation or aqueous-phase reactions. Indeed, the correlation coefficients of both nitrate

564 and organic Aitken mode MMDs with respect to sulfate were notably lower (0.50 and 0.62) indicating frequent periods

565 of particle populations with different species prevailing in different size regions within the Aitken mode.

566 Sulfate and nitrate were still more likely to occur internally mixed in the Aitken mode in spring with similar diameters

567 (nitrate to sulfate MMD ratio = 1.00), while organic Aitken mode MMDs were consistently lower, indicating greater

568 fractions of organic dominated particles towards the lower end and more inorganic dominated particles towards the

569 upper end of the fitted Aitken mode.

570 In summer, both nitrate and organic MMDs tended to be lower than those of sulfate (diameter ratios of 0.79 – 0.83)

571 but similar to each other, thus implying a shift to externally mixed populations of more nitrate and organic enhanced

572 and internally mixed smaller Aitken mode particles and sulfate dominated larger Aitken mode particles.

573 At the suburban HKUST site, accumulation mode MMDs of both nitrate and organics were generally quite similar to

574 those of sulfate with diameter ratios of 0.88 – 1.06. Compared to the urban site, correlation coefficients of nitrate and

575 sulfate were consistently lower (0.54 – 0.67) indicating a much greater frequency of time periods where sulfate and

576 nitrate dominated particles in the accumulation exhibited significantly different particle size distributions.

577 In winter, organic MMDs were consistently lower than those of sulfate and nitrate indicating a greater proportion of
578 externally mixed particle populations with organics enriched particles in the lower accumulation size range and
579 inorganic dominated particles in the larger accumulation size range. The least variability in particle size was observed
580 in the summer season where MMDs in both Aitken and accumulation mode displayed variations in relatively narrow
581 ranges between 200-250nm and 500-700nm, whereas in the remaining seasons time periods with particle populations
582 of lower MMD were more frequent, extending to MMDs as low as 100nm in the Aitken mode and 300nm in the
583 accumulation mode.
584 In the Aitken mode, mass median diameters overall were quite similar across species, with diameter ratios of organic
585 and nitrate distributions to those of sulfate in the range of 0.87 – 1.06, indicating that they generally covered a similar
586 size range. The temporal agreement was highly variable with correlation coefficients (R_{pr}) spanning from 0.21 to 0.75
587 indicating that Aitken mode particle populations at the suburban site were generally more diverse and likely influenced
588 by a greater range of particle formation and growth mechanisms compared to the urban Mong Kok site.
589
590
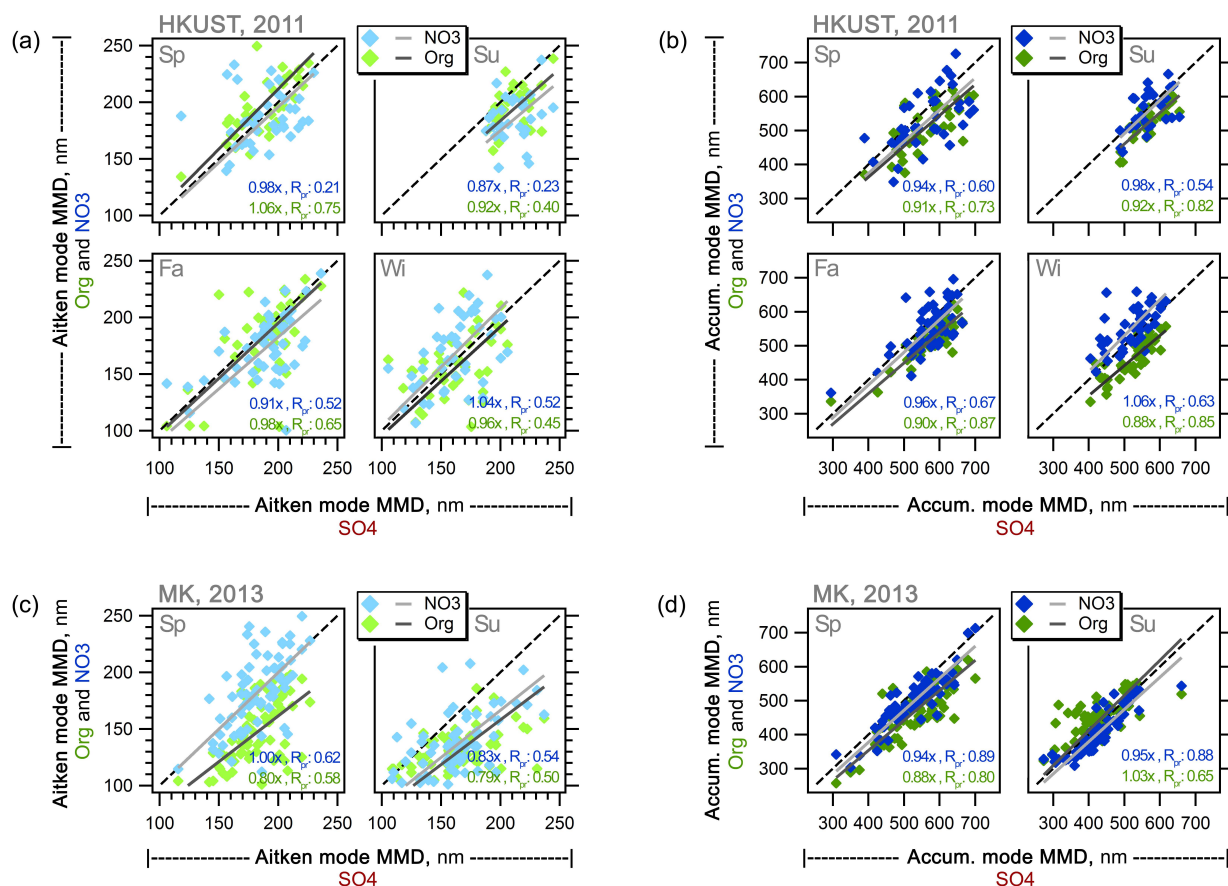
591
592 **Figure 6.** Scatter plots of fitted mass median diameters of organics and nitrate vs. sulfate for the (a) Aitken mode and (b)
593 accumulation mode at the HKUST suburban site, and (c) Aitken mode and (d) accumulation mode at the urban Mong Kok site

3.3. Comparison to previous studies

Particle size distribution studies in Hong Kong are generally scarce and have focused on either size segregated filter samples (MOUDI) for general ambient measurements or electrostatic classification in particle formation and particle growth studies (Guo et al., 2012;Cheung et al., 2015) . The latter studies focus on specific and narrow time periods and lack general discussions on ambient particle size distributions.

Two ambient studies were undertaken at the suburban coastal HKUST site using size-segregated samples from a ten-stage MOUDI sampler and offline chromatographic analysis. Inorganic constituents (NH4, NO3, SO4) in fine particles (i.e. D_p<1.8 µm) were shown to follow bimodal distributions with mode diameters in the range of 0.14-0.21 µm and 0.46-0.58 µm in samples collected in the winter season, while the main mode was observed in the coarse region (4-6 µm) for all three species (Zhuang et al., 1999). A subsequent year-long observational study also reported bimodal fine particle distributions with mode diameters of 0.1-0.3 µm and 0.7–0.9 µm and 1-2 additional modes in the coarse region (Bian et al., 2014), however, the main mode in the size distributions of sulfate, ammonium, potassium and oxalate was observed in the droplet mode ($0.7 - 0.9$ µm) in this study. Vehicle exhaust plumes sampled on-road from a Mobile Real-time Air Monitoring Platform (MAP) across Hong Kong's road network exhibited three distinct particle volume size distributions: a unimodal distribution with an accumulation mode at 0.2 µm and two bimodal distributions with a minor mode at 0.2 µm and the dominant mode at 0.5 or 0.7 µm (Yao et al., 2007a).

The bimodality in the fine particle range across these studies is consistent with the AMS-based results in this work. Nominally, the accumulation mode diameters from filter based studies and the chase studies are larger than those from AMS measurements where maximum mode diameters occurred at D_{va} ~ 700nm, corresponding to D_a ~ 470 (assuming D_{va} ~ D_a * density; particle density ~ 1.5 g/cm^3). Direct comparability is however limited due to fundamental differences in sizing techniques (MOUDI: atmospheric pressure; AMS: near-vacuum), sampling times (MOUDI: 24h samples, scattered time line; AMS: minute raw resolution averaged to hourly or daily, continuous time line), measurement uncertainties (MOUDI: sampling artifacts such as vapor adsorption and desorption; AMS: inlet lens transmission) and aerosol pretreatment (none for MOUDI with potential impacts on particle size in high humidity (>80%) conditions (Fang et al., 1991); AMS: removal of water prior to introduction to instrument).

3.4. Influence of AMS lens transmission

The quantitative measurement of particle components in the AMS is dependent on three major factors which may lead to particle loss prior to detection (Huffman et al., 2005). Irregularly shaped particles deviating from the flight path in the vacuum chamber may miss the vaporizer. Particles bouncing off the vaporizer surface will not be vaporized and hence may not be detected. Lastly, the aerodynamic lens which is part of the instrument's inlet system does not transmit particles uniformly across all particle diameters. Small particles are lost due to insufficient focusing or diffusion and large particle impact the lens apertures (Liu et al., 2007;Williams et al., 2013). Being a function of particle size, the latter factor affects both total AMS quantifiable particle mass (NR-PM$_1$) and measured mass size distributions. Transmission curves determined for the standard lens, which is fitted in most AMS instruments, can

629 vary but typically show efficient (i.e. close to 100%) transmission in the range of 100-550nm (Knote et al., 2011)

630 falling of significantly at either edge.

631 We examined the potential impact of lens transmission on the AMS mass size distributions on a number of 24h size

632 distributions from the fall season HKUST dataset covering both efficient and reduced lens transmission size regimes

633 (accumulation mode diameters between 400 and 600nm). Panels a-c in Figure D18 in the Supporting Material depict

634 original and lens-transmission corrected 24h mass size distributions for organic, nitrate and sulfate, assuming the

635 transmission function (subpanel d) reported by Liu et al., 2007. Impacts were generally larger in the accumulation

636 mode range with evident shifts to larger mode diameters and larger mode mass concentrations observed in all size

637 distributions. In the small diameter range, enhanced shoulders can occur which may however be artifacts due to the

638 larger uncertainties (low signal to noise ratio at small particle mass), i.e. greater noisiness at the leading end of AMS

639 size distributions. For a quantitative comparison, bimodal fitting parameters from the corrected distributions were

640 plotted against those from, the original distributions in Figure D18 in the Supporting Material (subpanels e-g refer to

641 the Aitken mode and subpanels h-j to the accumulation mode). Leading edge shoulders in the corrected size

642 distributions were not considered in the fitting. Changes in the Aitken mode mass median diameters were minor (on

643 average ~3%), while the integrated mode particle mass increased moderately (~48%). In the accumulation mode, mass

644 median diameters increased by ~28% and integrated mode particle mass doubled. The distribution widths (geometric

645 standard deviations) exhibited little change in both modes (increases of 2-3%).

646 Fitting results will therefore vary depending on whether AMS size distribution and concentration data are corrected

647 for lens transmission. While explicit lens transmission corrections can improve the accuracy of quantification of AMS

648 species concentration and size distribution measurements, few ambient studies explicitly use lens transmission

649 corrections based on individual experimental determinations or literature values e.g. (Quinn et al., 2006;Cross et al.,

650 2007). Lens transmission curves can vary between instruments (Fast et al., 2009) and are inherently difficult to

651 determine accurately experimentally. As discussed previously, scaling of size distributions by lens transmission curves

652 may introduce artifacts in noisier size distributions (e.g. low end of the Aitken mode, low concentration periods, short

653 term size distribution averages). Trailing edges from slow vaporization (e.g. under high particle mass loadings) may

654 be exacerbated and inflate mass concentrations at the upper size cut range of the AMS. The majority of ambient

655 studies employs a combined correction factor (collection efficiency, CE) considered to be the joint product of the

656 previously mentioned transmission efficiencies related to particle bounce, beam broadening and lens transmission

657 (Middlebrook et al., 2012) derived from aerosol composition and by comparison to collocated speciation or particle

658 sizing instruments. As the AMS lens transmission curve could not be determined in this study and to avoid additional

659 uncertainties from the application of non-instrument specific lens transmission values, we followed the CE correction

660 method in the analysis of the size distribution data in this study. The reported values of resolved mode diameters and

661 integrated mode should therefore be regarded as lower bound estimates in the context of the instrumental limitations

662 affecting ambient AMS measurements.

663

664

4. Conclusion

A detailed analysis of AMS mass-based particle size distributions of sulfate, nitrate, and organics in submicron particulate matter measured at two contrasting locations in Hong Kong during two field campaigns has been undertaken. Deconvolution of size distributions into Aitken and accumulation submodes was accomplished by log-normal peak fitting and trends in particle size (mass median diameters), dispersity (geometric standard deviation) and overall particle mass (integrated mode area) were discussed on a diurnal time scale and on a daily basis to evaluate longer-term changes in size distribution characteristics. At the urban roadside location, clear diurnal influences of primary particle and gas-phase species were evident affecting both inorganic and organic component size distributions. Traffic and cooking contributed an estimated $0.3 – 0.9 \, \mu g/m^3$ and $0.5 – 1.8 \, \mu g/m^3$ of organic component particle mass in the Aitken mode, and $1.6 - 1.8 \, \mu g/m^3$ and $1.0 – 2.7 \, \mu g/m^3$ respectively in the accumulation mode with concentrations level varying with seasons. Notable changes in Aitken mode mass median diameters of organics were limited to the morning rush hour. Daytime particle concentration maxima of sulfate and nitrate in summer indicated substantial influence of photochemical processes, which also led to increments in mass median diameters in the accumulation mode thus inferring associated particle growth. Nocturnal nitrate formation was apparent in the accumulation mode in spring concurring with the nighttime peak of ozone at the roadside, while in the Aitken mode nitrate particle concentrations were significantly elevated during the dinner hours. Organics-related size distributions were mostly governed by intra-day changes at the urban site with very similar trends across different size distribution sets (i.e. concentration regimes), while disparities in diurnal variations among different size distribution sets were evident for nitrate and sulfate, particularly affecting the average sets, indicating stronger influence of irregular external factors which were not associated with diurnal time scale processes.

Suburban particle size distributions exhibited variable diurnal characteristics, suggesting that irregular processes such as transport and seasonal meteorological conditions were the more dominant processes influencing particle size characteristics. Aitken mode particle mass of organics was significantly larger in spring and summer indicating greater influence of more local formation sources in the warm season. In the accumulation mode, organic particle mass concentrations were highest in fall and lowest in spring, following the frequency pattern of continental air mass influence. For sulfate, Aitken mode mass concentrations mass concentrations peaked in the afternoon from spring throughout fall with highest nominal concentrations in spring and summer and lowest levels in winter, while accumulation mode particle mass was highest in summer and fall and lowest in winter, similar to the trend observed among organic constituents.

Nitrate particle mass in the Aitken mode was generally small in most seasons ($0.01 - 0.06 \, \mu g/m^3$), except winter where daytime concentrations reached $\sim 0.1 \, \mu g/m^3$. In both modes, changes in mass median diameters varied temporally and in magnitude with seasons, indicating a stronger influence of specific meteorological conditions on the properties of nitrate-containing particles at the suburban site. At the urban site, periods of greater inorganic species mass concentrations were more likely to be caused by increases in both Aitken and accumulation mode particle mass in summer, indicating that particle formation and growth affecting smaller particles was more likely to occur in the warmer season. At the suburban receptor location, significant correlation of submode particle mass to total species concentration ($0.5 \leq R_{pr} \leq 0.7$) was observed for organics and nitrate in most seasons (spring, summer, winter)

702 suggesting notable influence of local or regional formation processes on organic and nitrate Aitken mode particulate

703 mass. Variations in particle mixing state were examined by evaluation of inter-species mass median diameter trends

704 at both measurement sites. In the accumulation mode at the urban site, internal mixing appeared to be prevalent in

705 spring, while greater frequency of time periods with external mixing of particle populations comprising different

706 fractions of organic constituents was observed in summer. External mixing was predominant in the Aitken mode at

707 the urban location in both seasons. At the suburban site, sulfate and nitrate in the accumulation mode more frequently

708 exhibited differing particle size distributions in all seasons signifying a greater extent of external mixing. In winter,

709 external mixing of more organics enriched particles in the lower accumulation size range was evident.

710 Acknowledgements

711 This work was supported by the Environmental Conservation Fund of Hong Kong (project number ECWW09EG04).

712 Chak K. Chan gratefully acknowledges the startup fund of the City University of Hong Kong.

713 References

714 Abbatt, J. P. D., Broekhuizen, K., and Pradeep Kumar, P.: Cloud condensation nucleus activity of internally mixed

715   ammonium sulfate/organic acid aerosol particles, Atmospheric Environment, 39, 4767-4778,

716   10.1016/j.atmosenv.2005.04.029, 2005.

717 Ahlquist, N. C., and Charlson, R. J.: A New Instrument for Evaluating the Visual Quality of Air, Journal of the Air

718   Pollution Control Association, 17, 467-469, 10.1080/00022470.1967.10469006, 1967.

719 Aiken, A. C., Salcedo, D., Cubison, M. J., Huffman, J. A., DeCarlo, P. F., Ulbrich, I. M., Docherty, K. S., Sueper,

720   D., Kimmel, J. R., Worsnop, D. R., Trimborn, A., Northway, M., Stone, E. A., Schauer, J. J., Volkamer, R. M.,

721   Fortner, E., de Foy, B., Wang, J., Laskin, A., Shutthanandan, V., Zheng, J., Zhang, R., Gaffney, J., Marley, N.

722   A., Paredes-Miranda, G., Arnott, W. P., Molina, L. T., Sosa, G., and Jimenez, J. L.: Mexico City aerosol

723   analysis during MILAGRO using high resolution aerosol mass spectrometry at the urban supersite (T0) - Part 1:

724   Fine particle composition and organic source apportionment, Atmospheric Chemistry and Physics, 9, 6633-

725   6653, 2009.

726 Bahreini, R., Dunlea, E. J., Matthew, B. M., Simons, C., Docherty, K. S., DeCarlo, P. F., Jimenez, J. L., Brock, C.

727   A., and Middlebrook, A. M.: Design and Operation of a Pressure-Controlled Inlet for Airborne Sampling with

728   an Aerodynamic Aerosol Lens, Aerosol Science and Technology, 42, 465-471, 10.1080/02786820802178514,

729   2008.

730 Bian, Q., Huang, X. H. H., and Yu, J. Z.: One-year observations of size distribution characteristics of major aerosol

731   constituents at a coastal receptor site in Hong Kong – Part 1: Inorganic ions and oxalate, Atmos. Chem.

732   Phys., 14, 9013-9027, 10.5194/acp-14-9013-2014, 2014.

733 Bohren, C. F., and Huffman, D. R.: Absorption and scattering of light by small particles, in: Absorption and

734   Scattering of Light by Small Particles, Wiley-VCH Verlag GmbH, 1-11, 1983.

735 Canagaratna, M. R., Jayne, J. T., Jimenez, J. L., Allan, J. D., Alfarra, M. R., Zhang, Q., Onasch, T. B., Drewnick, F.,
736   Coe, H., Middlebrook, A., Delia, A., Williams, L. R., Trimborn, A. M., Northway, M. J., DeCarlo, P. F., Kolb,
737   C. E., Davidovits, P., and Worsnop, D. R.: Chemical and microphysical characterization of ambient aerosols
738   with the aerodyne aerosol mass spectrometer, Mass Spectrometry Reviews, 26, 185-222, 10.1002/mas.20115,
739   2007.
740 Charlson, R. J., Langner, J., Rodhe, H., Leovy, C. B., and Warren, S. G.: Perturbation of the northern hemisphere
741   radiative balance by backscattering from anthropogenic sulfate aerosols*, Tellus B, 43, 152-163,
742   10.1034/j.1600-0889.1991.t01-1-00013.x, 1991.
743 Cheung, K., Ling, Z. H., Wang, D. W., Wang, Y., Guo, H., Lee, B., Li, Y. J., and Chan, C. K.: Characterization and
744   source identification of sub-micron particles at the HKUST Supersite in Hong Kong, Science of The Total
745   Environment, 527–528, 287-296, http://dx.doi.org/10.1016/j.scitotenv.2015.04.087, 2015.
746 Crippa, M., DeCarlo, P. F., Slowik, J. G., Mohr, C., Heringa, M. F., Chirico, R., Poulain, L., Freutel, F., Sciare, J.,
747   Cozic, J., Di Marco, C. F., Elsasser, M., Nicolas, J. B., Marchand, N., Abidi, E., Wiedensohler, A., Drewnick,
748   F., Schneider, J., Borrmann, S., Nemitz, E., Zimmermann, R., Jaffrezo, J. L., Prévôt, A. S. H., and
749   Baltensperger, U.: Wintertime aerosol chemical composition and source apportionment of the organic fraction
750   in the metropolitan area of Paris, Atmos. Chem. Phys., 13, 961-981, 10.5194/acp-13-961-2013, 2013.
751 Cross, E. S., Slowik, J. G., Davidovits, P., Allan, J. D., Worsnop, D. R., Jayne, J. T., Lewis †, D. K., Canagaratna,
752   M., and Onasch, T. B.: Laboratory and Ambient Particle Density Determinations using Light Scattering in
753   Conjunction with Aerosol Mass Spectrometry, Aerosol Science and Technology, 41, 343-359,
754   10.1080/02786820701199736, 2007.
755 Cross, E. S., Onasch, T. B., Canagaratna, M., Jayne, J. T., Kimmel, J., Yu, X. Y., Alexander, M. L., Worsnop, D. R.,
756   and Davidovits, P.: Single particle characterization using a light scattering module coupled to a time-of-flight
757   aerosol mass spectrometer, Atmos. Chem. Phys., 9, 7769-7793, 10.5194/acp-9-7769-2009, 2009.
758 Davidson, C. I., Phalen, R. F., and Solomon, P. A.: Airborne Particulate Matter and Human Health: A Review,
759   Aerosol Science and Technology, 39, 737-749, 10.1080/02786820500191348, 2005.
760 DeCarlo, P. F., Slowik, J. G., Worsnop, D. R., Davidovits, P., and Jimenez, J. L.: Particle morphology and density
761   characterization by combined mobility and aerodynamic diameter measurements. Part 1: Theory, Aerosol
762   Science and Technology, 38, 1185-1205, 10.1080/027868290903907, 2004.
763 Docherty, K. S., Aiken, A. C., Huffman, J. A., Ulbrich, I. M., DeCarlo, P. F., Sueper, D., Worsnop, D. R., Snyder,
764   D. C., Peltier, R. E., Weber, R. J., Grover, B. D., Eatough, D. J., Williams, B. J., Goldstein, A. H., Ziemann, P.
765   J., and Jimenez, J. L.: The 2005 Study of Organic Aerosols at Riverside (SOAR-1): instrumental
766   intercomparisons and fine particle composition, Atmospheric Chemistry and Physics, 11, 12387-12420,
767   10.5194/acp-11-12387-2011, 2011.
768 Docherty, K. S., Lewandowski, M., and Jimenez, J. L.: Effect of Vaporizer Temperature on Ambient Non-
769   Refractory Submicron Aerosol Composition and Mass Spectra Measured by the Aerosol Mass Spectrometer,
770   Aerosol Science and Technology, 49, 485-494, 10.1080/02786826.2015.1042100, 2015.

771   Drewnick, F., Hings, S. S., DeCarlo, P., Jayne, J. T., Gonin, M., Fuhrer, K., Weimer, S., Jimenez, J. L., Demerjian,
772   K. L., Borrmann, S., and Worsnop, D. R.: A new time-of-flight aerosol mass spectrometer (TOF-AMS) -
773   Instrument description and first field deployment, Aerosol Science and Technology, 39, 637-658,
774   10.1080/02786820500182040, 2005.

775   Elser, M., Huang, R. J., Wolf, R., Slowik, J. G., Wang, Q., Canonaco, F., Li, G., Bozzetti, C., Daellenbach, K. R.,
776   Huang, Y., Zhang, R., Li, Z., Cao, J., Baltensperger, U., El-Haddad, I., and Prévôt, A. S. H.: New insights into
777   PM2.5 chemical composition and sources in two major cities in China during extreme haze events using aerosol
778   mass spectrometry, Atmos. Chem. Phys., 16, 3207-3225, 10.5194/acp-16-3207-2016, 2016.

779   Farmer, D. K., Matsunaga, A., Docherty, K. S., Surratt, J. D., Seinfeld, J. H., Ziemann, P. J., and Jimenez, J. L.:
780   Response of an aerosol mass spectrometer to organonitrates and organosulfates and implications for
781   atmospheric chemistry, Proceedings of the National Academy of Sciences of the United States of America, 107,
782   6670-6675, 10.1073/pnas.0912340107, 2010.

783   Fast, J., Aiken, A. C., Allan, J., Alexander, L., Campos, T., Canagaratna, M. R., Chapman, E., DeCarlo, P. F., de
784   Foy, B., Gaffney, J., de Gouw, J., Doran, J. C., Emmons, L., Hodzic, A., Herndon, S. C., Huey, G., Jayne, J. T.,
785   Jimenez, J. L., Kleinman, L., Kuster, W., Marley, N., Russell, L., Ochoa, C., Onasch, T. B., Pekour, M., Song,
786   C., Ulbrich, I. M., Warneke, C., Welsh-Bon, D., Wiedinmyer, C., Worsnop, D. R., Yu, X. Y., and Zaveri, R.:
787   Evaluating simulated primary anthropogenic and biomass burning organic aerosols during MILAGRO:
788   implications for assessing treatments of secondary organic aerosols, Atmospheric Chemistry and Physics, 9,
789   6191-6215, 2009.

790   Gill, P. E., Murray, W., and Wright, M. H.: The Levenberg-Marquardt method, in: Practical optimization, Academic
791   Press, London, 1981.

792   Griffith, S. M., Huang, X. H. H., Louie, P. K. K., and Yu, J. Z.: Characterizing the thermodynamic and chemical
793   composition factors controlling PM2.5 nitrate: Insights gained from two years of online measurements in Hong
794   Kong, Atmospheric Environment, 122, 864-875, http://dx.doi.org/10.1016/j.atmosenv.2015.02.009, 2015.

795   Guo, H., Wang, D. W., Cheung, K., Ling, Z. H., Chan, C. K., and Yao, X. H.: Observation of aerosol size
796   distribution and new particle formation at a mountain site in subtropical Hong Kong, Atmos. Chem. Phys., 12,
797   9923-9939, 10.5194/acp-12-9923-2012, 2012.

798   Huang, X. F., He, L. Y., Hu, M., Canagaratna, M. R., Sun, Y., Zhang, Q., Zhu, T., Xue, L., Zeng, L. W., Liu, X. G.,
799   Zhang, Y. H., Jayne, J. T., Ng, N. L., and Worsnop, D. R.: Highly time-resolved chemical characterization of
800   atmospheric submicron particles during 2008 Beijing Olympic Games using an Aerodyne High-Resolution
801   Aerosol Mass Spectrometer, Atmospheric Chemistry and Physics, 10, 8933-8945, 10.5194/acp-10-8933-2010,
802   2010.

803   Huang, X. F., He, L. Y., Hu, M., Canagaratna, M. R., Kroll, J. H., Ng, N. L., Zhang, Y. H., Lin, Y., Xue, L., Sun, T.
804   L., Liu, X. G., Shao, M., Jayne, J. T., and Worsnop, D. R.: Characterization of submicron aerosols at a rural site
805   in Pearl River Delta of China using an Aerodyne High-Resolution Aerosol Mass Spectrometer, Atmospheric
806   Chemistry and Physics, 11, 1865-1877, 10.5194/acp-11-1865-2011, 2011.

807   Huang, X. H. H., Bian., Q. J., Ng, W. M., Louie, P. K. K., and Yu, J. Z.: Characterization of PM2.5 Major
808   Components and Source Investigation in Suburban Hong Kong: A One Year Monitoring Study, Aerosol and Air
809   Quality Research 14, 237-250, 2014.
810   Huffman, J. A., Jayne, J. T., Drewnick, F., Aiken, A. C., Onasch, T., Worsnop, D. R., and Jimenez, J. L.: Design,
811   modeling, optimization, and experimental tests of a particle beam width probe for the aerodyne aerosol mass
812   spectrometer, Aerosol Science and Technology, 39, 1143-1163, 10.1080/02786820500423782, 2005.
813   Jayne, J. T., Leard, D. C., Zhang, X. F., Davidovits, P., Smith, K. A., Kolb, C. E., and Worsnop, D. R.:
814   Development of an aerosol mass spectrometer for size and composition analysis of submicron particles, Aerosol
815   Science and Technology, 33, 49-70, 2000.
816   Jimenez, J. L., Jayne, J. T., Shi, Q., Kolb, C. E., Worsnop, D. R., Yourshaw, I., Seinfeld, J. H., Flagan, R. C., Zhang,
817   X., Smith, K. A., Morris, J. W., and Davidovits, P.: Ambient aerosol sampling using the Aerodyne Aerosol
818   Mass Spectrometer, J. Geophys. Res., 108, 8425, 10.1029/2001jd001213, 2003.
819   John, W.: Size Distribution Characteristics of Aerosols, in: Aerosol Measurement, John Wiley & Sons, Inc., 41-54,
820   2011.
821   Kerminen, V. M., Paramonov, M., Anttila, T., Riipinen, I., Fountoukis, C., Korhonen, H., Asmi, E., Laakso, L.,
822   Lihavainen, H., Swietlicki, E., Svenningsson, B., Asmi, A., Pandis, S. N., Kulmala, M., and Petäjä, T.: Cloud
823   condensation nuclei production associated with atmospheric nucleation: a synthesis based on existing literature
824   and new results, Atmos. Chem. Phys., 12, 12037-12059, 10.5194/acp-12-12037-2012, 2012.
825   Knote, C., Brunner, D., Vogel, H., Allan, J., Asmi, A., Äijälä, M., Carbone, S., van der Gon, H. D., Jimenez, J. L.,
826   Kiendler-Scharr, A., Mohr, C., Poulain, L., Prévôt, A. S. H., Swietlicki, E., and Vogel, B.: Towards an online-
827   coupled chemistry-climate model: evaluation of trace gases and aerosols in COSMO-ART, Geosci. Model Dev.,
828   4, 1077-1102, 10.5194/gmd-4-1077-2011, 2011.
829   Köhler, H.: The nucleus in and the growth of hygroscopic droplets, Transactions of the Faraday Society, 32, 1152-
830   1161, 10.1039/tf9363201152, 1936.
831   Lee, B. P., Li, Y. J., Yu, J. Z., Louie, P. K. K., and Chan, C. K.: Physical and chemical characterization of ambient
832   aerosol by HR-ToF-AMS at a suburban site in Hong Kong during springtime 2011, Journal of Geophysical
833   Research: Atmospheres, 118, 8625-8639, 10.1002/jgrd.50658, 2013.
834   Lee, B. P., Li, Y. J., Yu, J. Z., Louie, P. K. K., and Chan, C. K.: Characteristics of submicron particulate matter at
835   the urban roadside in downtown Hong Kong—Overview of 4 months of continuous high-resolution aerosol
836   mass spectrometer measurements, Journal of Geophysical Research: Atmospheres, 120, 7040-7058,
837   10.1002/2015JD023311, 2015.
838   Li, Y. J., Lee, B. Y. L., Yu, J. Z., Ng, N. L., and Chan, C. K.: Evaluating the degree of oxygenation of organic
839   aerosol during foggy and hazy days in Hong Kong using high-resolution time-of-flight aerosol mass
840   spectrometry (HR-ToF-AMS), Atmos. Chem. Phys., 13, 8739-8753, 10.5194/acp-13-8739-2013, 2013.
841   Li, Y. J., Lee, B. P., Su, L., Fung, J. C. H., and Chan, C. K.: Seasonal characteristics of fine particulate matter (PM)
842   based on high resolution time-of-flight aerosol mass spectrometric (HR-ToF-AMS) measurements at the
843   HKUST Supersite in Hong Kong, Atmos. Chem. Phys., 15, 37-53, doi:10.5194/acp-15-37-2015, 2015.

844   Liu, P. S. K., Deng, R., Smith, K. A., Williams, L. R., Jayne, J. T., Canagaratna, M. R., Moore, K., Onasch, T. B.,

845   Worsnop, D. R., and Deshler, T.: Transmission efficiency of an aerodynamic focusing lens system: Comparison

846   of model calculations and laboratory measurements for the Aerodyne Aerosol Mass Spectrometer, Aerosol

847   Science and Technology, 41, 721-733, 10.1080/02786820701422278, 2007.

848   Man, H., Zhu, Y., Ji, F., Yao, X., Lau, N. T., Li, Y., Lee, B. P., and Chan, C. K.: Comparison of Daytime and

849   Nighttime New Particle Growth at the HKUST Supersite in Hong Kong, Environmental Science & Technology,

850   49, 7170-7178, 10.1021/acs.est.5b02143, 2015.

851   Meng, J. W., Yeung, M. C., Li, Y. J., Lee, B. Y. L., and Chan, C. K.: Size-resolved cloud condensation nuclei

852   (CCN) activity and closure analysis at the HKUST Supersite in Hong Kong, Atmos. Chem. Phys., 14, 10267-

853   10282, 10.5194/acp-14-10267-2014, 2014.

854   Middlebrook, A. M., Bahreini, R., Jimenez, J. L., and Canagaratna, M. R.: Evaluation of Composition-Dependent

855   Collection Efficiencies for the Aerodyne Aerosol Mass Spectrometer using Field Data, Aerosol Science and

856   Technology, 46, 258-271, 10.1080/02786826.2011.620041, 2012.

857   Mohr, C., DeCarlo, P. F., Heringa, M. F., Chirico, R., Slowik, J. G., Richter, R., Reche, C., Alastuey, A., Querol, X.,

858   Seco, R., Peñuelas, J., Jiménez, J. L., Crippa, M., Zimmermann, R., Baltensperger, U., and Prévôt, A. S. H.:

859   Identification and quantification of organic aerosol from cooking and other sources in Barcelona using aerosol

860   mass spectrometer data, Atmos. Chem. Phys., 12, 1649-1665, 10.5194/acp-12-1649-2012, 2012.

861   Quinn, P. K., Bates, T. S., Coffman, D., Onasch, T. B., Worsnop, D., Baynard, T., de Gouw, J. A., Goldan, P. D.,

862   Kuster, W. C., Williams, E., Roberts, J. M., Lerner, B., Stohl, A., Pettersson, A., and Lovejoy, E. R.: Impacts of

863   sources and aging on submicrometer aerosol properties in the marine boundary layer across the Gulf of Maine,

864   J. Geophys. Res., 111, D23S36, 10.1029/2006jd007582, 2006.

865   Rupakheti, M., Leaitch, W. R., Lohmann, U., Hayden, K., Brickell, P., Lu, G., Li, S. M., Toom-Sauntry, D.,

866   Bottenheim, J. W., Brook, J. R., Vet, R., Jayne, J. T., and Worsnop, D. R.: An intensive study of the size and

867   composition of submicron atmospheric aerosols at a rural site in Ontario, Canada, Aerosol Science and

868   Technology, 39, 722-736, 10.1080/02786820500182420, 2005.

869   Saarikoski, S., Carbone, S., Decesari, S., Giulianelli, L., Angelini, F., Canagaratna, M., Ng, N. L., Trimborn, A.,

870   Facchini, M. C., Fuzzi, S., Hillamo, R., and Worsnop, D.: Chemical characterization of springtime

871   submicrometer aerosol in Po Valley, Italy, Atmos. Chem. Phys., 12, 8401-8421, 10.5194/acp-12-8401-2012,

872   2012.

873   Salcedo, D., Onasch, T. B., Dzepina, K., Canagaratna, M. R., Zhang, Q., Huffman, J. A., DeCarlo, P. F., Jayne, J. T.,

874   Mortimer, P., Worsnop, D. R., Kolb, C. E., Johnson, K. S., Zuberi, B., Marr, L. C., Volkamer, R., Molina, L. T.,

875   Molina, M. J., Cardenas, B., Bernabe, R. M., Marquez, C., Gaffney, J. S., Marley, N. A., Laskin, A.,

876   Shutthanandan, V., Xie, Y., Brune, W., Lesher, R., Shirley, T., and Jimenez, J. L.: Characterization of ambient

877   aerosols in Mexico City during the MCMA-2003 campaign with Aerosol Mass Spectrometry: results from the

878   CENICA Supersite, Atmospheric Chemistry and Physics, 6, 925-946, 2006.

879   Schwartz, S. E.: The whitehouse effect—Shortwave radiative forcing of climate by anthropogenic aerosols: an

880   overview, Journal of Aerosol Science, 27, 359-382, http://dx.doi.org/10.1016/0021-8502(95)00533-1, 1996.

881 Seinfeld, J. H., and Pandis, S. N.: Atmospheric Chemistry and Physics - From Air Pollution to Climate Change (2nd
882   Edition). John Wiley & Sons, 2006.

883 Setyan, A., Zhang, Q., Merkel, M., Knighton, W. B., Sun, Y., Song, C., Shilling, J. E., Onasch, T. B., Herndon, S.
884   C., Worsnop, D. R., Fast, J. D., Zaveri, R. A., Berg, L. K., Wiedensohler, A., Flowers, B. A., Dubey, M. K., and
885   Subramanian, R.: Characterization of submicron particles influenced by mixed biogenic and anthropogenic
886   emissions using high-resolution aerosol mass spectrometry: results from CARES, Atmos. Chem. Phys., 12,
887   8131-8156, 10.5194/acp-12-8131-2012, 2012.

888 Slowik, J. G., Stainken, K., Davidovits, P., Williams, L. R., Jayne, J. T., Kolb, C. E., Worsnop, D. R., Rudich, Y.,
889   DeCarlo, P. F., and Jimenez, J. L.: Particle morphology and density characterization by combined mobility and
890   aerodynamic diameter measurements. Part 2: Application to combustion-generated soot aerosols as a function of
891   fuel equivalence ratio, Aerosol Science and Technology, 38, 1206-1222, 10.1080/027868290903916, 2004.

892 Sun, C., Lee, B. P., Huang, D., Jie Li, Y., Schurman, M. I., Louie, P. K. K., Luk, C., and Chan, C. K.: Continuous
893   measurements at the urban roadside in an Asian megacity by Aerosol Chemical Speciation Monitor (ACSM):
894   particulate matter characteristics during fall and winter seasons in Hong Kong, Atmos. Chem. Phys., 16, 1713-
895   1728, 10.5194/acp-16-1713-2016, 2016.

896 Sun, Y., Zhang, Q., Macdonald, A. M., Hayden, K., Li, S. M., Liggio, J., Liu, P. S. K., Anlauf, K. G., Leaitch, W.
897   R., Steffen, A., Cubison, M., Worsnop, D. R., van Donkelaar, A., and Martin, R. V.: Size-resolved aerosol
898   chemistry on Whistler Mountain, Canada with a high-resolution aerosol mass spectrometer during INTEX-B,
899   Atmos. Chem. Phys., 9, 3095-3111, 10.5194/acp-9-3095-2009, 2009.

900 Sun, Y. L., Zhang, Q., Schwab, J. J., Demerjian, K. L., Chen, W. N., Bae, M. S., Hung, H. M., Hogrefe, O., Frank,
901   B., Rattigan, O. V., and Lin, Y. C.: Characterization of the sources and processes of organic and inorganic
902   aerosols in New York city with a high-resolution time-of-flight aerosol mass apectrometer, Atmospheric
903   Chemistry and Physics, 11, 1581-1602, 10.5194/acp-11-1581-2011, 2011.

904 Takegawa, N., Miyakawa, T., Watanabe, M., Kondo, Y., Miyazaki, Y., Han, S., Zhao, Y., van Pinxteren, D.,
905   Bruggemann, E., Gnauk, T., Herrmann, H., Xiao, R., Deng, Z., Hu, M., Zhu, T., and Zhang, Y.: Performance of
906   an Aerodyne Aerosol Mass Spectrometer (AMS) during Intensive Campaigns in China in the Summer of 2006,
907   Aerosol Science and Technology, 43, 189-204, 10.1080/02786820802582251, 2009.

908 Ulbrich, I. M., Canagaratna, M. R., Cubison, M. J., Zhang, Q., Ng, N. L., Aiken, A. C., and Jimenez, J. L.: Three-
909   dimensional factorization of size-resolved organic aerosol mass spectra from Mexico City, Atmos. Meas. Tech.,
910   5, 195-224, 10.5194/amt-5-195-2012, 2012.

911 Westervelt, D. M., Pierce, J. R., Riipinen, I., Trivitayanurak, W., Hamed, A., Kulmala, M., Laaksonen, A., Decesari,
912   S., and Adams, P. J.: Formation and growth of nucleated particles into cloud condensation nuclei: model–
913   measurement comparison, Atmos. Chem. Phys., 13, 7645-7663, 10.5194/acp-13-7645-2013, 2013.

914 Williams, L. R., Gonzalez, L. A., Peck, J., Trimborn, D., McInnis, J., Farrar, M. R., Moore, K. D., Jayne, J. T.,
915   Robinson, W. A., Lewis, D. K., Onasch, T. B., Canagaratna, M. R., Trimborn, A., Timko, M. T., Magoon, G.,
916   Deng, R., Tang, D., de la Rosa Blanco, E., Prévôt, A. S. H., Smith, K. A., and Worsnop, D. R.: Characterization

917   of an aerodynamic lens for transmitting particles greater than 1 micrometer in diameter into the Aerodyne

918   aerosol mass spectrometer, Atmos. Meas. Tech., 6, 3271-3280, 10.5194/amt-6-3271-2013, 2013.

919 Yao, X., Lau, N. T., Chan, C. K., and Fang, M.: Size distributions and condensation growth of submicron particles

920   in on-road vehicle plumes in Hong Kong, Atmospheric Environment, 41, 3328-3338,

921   10.1016/j.atmosenv.2006.12.044, 2007a.

922 Yao, X., Ling, T. Y., Fang, M., and Chan, C. K.: Size dependence of in situ pH in submicron atmospheric particles

923   in Hong Kong, Atmospheric Environment, 41, 382-393, 10.1016/j.atmosenv.2006.07.037, 2007b.

924 Yuan, Z., Yadav, V., Turner, J. R., Louie, P. K. K., and Lau, A. K. H.: Long-term trends of ambient particulate

925   matter emission source contributions and the accountability of control strategies in Hong Kong over 1998–2008,

926   Atmospheric Environment, 76, 21-31, http://dx.doi.org/10.1016/j.atmosenv.2012.09.026, 2013.

927 Zhang, J. K., Sun, Y., Liu, Z. R., Ji, D. S., Hu, B., Liu, Q., and Wang, Y. S.: Characterization of submicron aerosols

928   during a month of serious pollution in Beijing, 2013, Atmos. Chem. Phys., 14, 2887-2903, 10.5194/acp-14-

929   2887-2014, 2014.

930 Zhang, Q., Stanier, C. O., Canagaratna, M. R., Jayne, J. T., Worsnop, D. R., Pandis, S. N., and Jimenez, J. L.:

931   Insights into the chemistry of new particle formation and growth events in Pittsburgh based on aerosol mass

932   spectrometry, Environmental Science & Technology, 38, 4797-4809, 10.1021/es035417u, 2004.

933 Zhang, Q., Canagaratna, M. R., Jayne, J. T., Worsnop, D. R., and Jimenez, J. L.: Time- and size-resolved chemical

934   composition of submicron particles in Pittsburgh: Implications for aerosol sources and processes, Journal of

935   Geophysical Research-Atmospheres, 110, D07s09 Artn d07s09, 2005.

936 Zheng, M., Kester, D. R., Wang, F., Shi, X., and Guo, Z.: Size distribution of organic and inorganic species in Hong

937   Kong aerosols during the wet and dry seasons, J. Geophys. Res., 113, D16303, 10.1029/2007jd009494, 2008.

938 Zhuang, H., Chan, C. K., Fang, M., and Wexler, A. S.: Size distributions of particulate sulfate, nitrate, and

939   ammonium at a coastal site in Hong Kong, Atmospheric Environment, 33, 843-853, 10.1016/s1352-

940   2310(98)00305-7, 1999.